P 74

ROTATING REACTOR STUDIES

Final Report

RAI-89-RR-2

Purchase Order H-80505B

Period Covered:

3/27/89 - 9/27/90

Prepared for:

George C. Marshall Space Flight Center

MSFC, AL 35812

Prepared by:

Dr. Glyn O. Roberts

Date:

January 10, 1991

Roberts Associates, Incorporated

380 West Maple Avenue, Suite L-1A

Vienna, VA 22180-5616

(NASA-CR-~~[illegible]~~ 184095) ROTATING REACTOR STUDIES Final Report, 27 Mar. 1989 - 27 Sep. 1990 (Roberts Associates) 74 p CSCL 22A

N91-1[illegible]

Unclas

[illegible] 0325[illegible]

Roberts Associates, Incorporated
380 West Maple Avenue, Suite L-1A
Vienna, VA 22180-5616
(703)242-2115 or (703)356-6630

January 10, 1991

Procurement Office
Code AP29F
MSFC, AL 35812

Subject: Final Report on Purchase Order H-80505B

Dear Sirs,

We are pleased to submit the subject report. The distribution list is that required by the order.

Yours sincerely,

Dr. Glyn O. Roberts
President

Distribution:
AP29-F (letter of transmittal only)
CN24D (5)
AT01
CC01/Wofford
EM13A-27
ES76/Snyder (1 + repro.)
NASA/STIF (1 + repro.)

TABLE OF CONTENTS

Abstract.....1
1. Introduction.....2
1.1 Background.....2
1.2 Applications.....2
1.3 Requirements.....3
1.4 Subjects for Analysis.....3
1.5 Methods of Study.....4
2. Results.....5
2.1 Experiments with Polystyrene Latex Microspheres.....5
2.2 Theory of the Secondary Flows.....6
2.3 Computer Solution for Uniform Rotation.....7
2.4 Report on Uniform-Rotation Theory.....9
3. Recommendations.....12
Acknowledgements.....12
References.....13
Appendix A. Viscosity Formulation for Water.....14
Appendix B. Solution of the Cubic Equation for Delta.....17
Appendix C. The ROTREAC Computer Program.....21
Appendix D. Particle Orbits in a Rotating Liquid.....30

LIST OF FIGURES

Figure 1. Reactor Cross Section with the Inner and Outer Circles.....10
Figure 2. Sample Plot for Radius Ratios as Functions of Rotation Rate.....11

Abstract

Undesired gravitational effects such as convection or sedimentation in a fluid can sometimes be avoided or decreased by the use of a closed chamber uniformly rotated about a horizontal axis.

In a previous study (Roberts, Kornfeld and Fowlis, 1989) we determined the spiral orbits of a heavy or buoyant particle in a uniformly rotating fluid. The particles move in circles, and spiral in or out under the combined effects of the centrifugal force and centrifugal buoyancy. We also formulated and solved an optimization problem for the rotation rate of a cylindrical reactor rotated about its axis and containing distributed particles.

This report is concerned with related studies in several areas.

We have upgraded a computer program based on our analysis, correcting some minor errors, adding a sophisticated screen-and-printer graphics capability and other output options, and improving the automation.

We have supported the design, performance, and analysis of a series of experiments with monodisperse polystyrene latex microspheres in water, to test the theory and its limitations.

The theory was amply confirmed at high rotation rates. But at low rotation rates (1rpm or less) the assumption of uniform solid-body rotation of the fluid became invalid, and there were increasingly strong secondary motions driven by variations in the mean fluid density due to variations in the particle concentration. In these tests the increase in the mean fluid density due to the particles was of order 0.015%.

To a first approximation, these flows are driven by the buoyancy in a thin crescent-shaped depleted layer on the descending side of the rotating reactor. This buoyancy distribution is balanced by viscosity near the walls, and by the Coriolis force in the interior. A full analysis is beyond the scope of this study.

Secondary flows are likely to be stronger for buoyant particles, which spiral in towards the neutral point near the rotation axis under the influence of their centrifugal buoyancy. This is because the depleted layer is thicker, and extends all the way around the reactor.

Section 1

INTRODUCTION

1.1 Background

The effects of particle or cell sedimentation in a fluid can be minimized by rotating the fluid container about a horizontal axis. The container itself need not necessarily be axisymmetric.

The technique has been used for experiments and for materials processing. It is useful alone, and as a preliminary to microgravity experiments in space.

If the fluid rotates uniformly with its container, then individual particles move in circular orbits, with the same rotation rate, about a center displaced horizontally from the axis of rotation. For particles at this center, their sedimentation velocity just cancels the upward or downward flow of the surrounding fluid. For particles denser than the fluid, the orbit radius increases slowly with time due to the net centrifugal force, so that the particles spiral outward from their center. Buoyant particles spiral inwards, due to the net buoyancy force.

Relative to rotating axes fixed to the container and fluid, all the particles with a given sedimentation rate move in phase, in circular orbits with a fixed radius equal to the separation between the axis and the center described above. The velocity of every particle is its sedimentation rate, in the current direction of gravity. This circular motion is superposed on a centrifugal motion away from or towards the axis. Particles with larger sedimentation rates move in larger circles.

1.2 Applications

The technique has been used in the following applications, among others:

Production of latex microspheres of uniform size;

Study microgravity effects on cells and tissue; and

Minimize gravitational flow disturbances in free-flow isoelectric focusing.

Other potential applications include crystal growth (where convection is sometimes a problem).

The alternatives of microgravity processing in space flight, in a plane flown on a parabolic flight path, or in a drop tower, are generally either too inconvenient and expensive, or too brief.

1.3 Requirements

Successful use of this technique in regard to particle processing (as for latex) imposes the following requirements:

Keep particles from collecting at container boundary before processing;

Keep particles from collecting at container boundary during processing;

Selective withdrawal of particles after processing, to exclude those that have interacted (or interacted excessively) with the container boundaries; and

Temperature control, where cells, tissues, or processes require it.

In addition, it is necessary to determine and increase any upper limits on the particle concentration that can be processed without seriously modifying the flow.

1.4 Subjects for Analysis

Experimental and theoretical study is needed in regard to the following questions, among others:

What happens to particles that hit the container boundary?

Are non-axisymmetric containers useful? For cylinders, what size and aspect ratio is appropriate?

Can useful flows be established during initialization by changes in the rotation rate? These spin-up and spin-down effects are dominated by the Coriolis force.

How is the mean flow modified by the aggregate net weight of the particle distribution? At what stage does this modification become a problem? An example of a related study is the work of Batchelor and Janse Van Rensburg on bidisperse sedimentation (1986).

1.5 Methods of Study

These problems should be studied using an appropriate combination of experiments, analytic methods, and computer models. A close interaction between these approaches is appropriate.

Analytic methods include solving ordinary differential equation systems (as for orbits, cf. Roberts et al. 1989), or partial differential equations (linearized calculations of rotating flows using a balance of buoyancy, viscosity forces, and pressure gradients).

Computer models are generally required when the problems are too hard for analytic methods. Our Atmospheric General Circulation Experiment (AGCE) computer code, developed under MSFC sponsorship, has great flexibility in the study of a wide range of rotating flows, with or without temperature variation, and has previously been applied to spin-up and to the isoelectric focusing case described above. In the limited scope of this program, computer modeling was limited to orbit calculations.

Frequent interaction with laboratory workers and involvement in the experiments should be a part of every such study. Our practice has been to maintain a close relationship with the laboratory workers, and to support the design of the equipment, the choice of the experimental procedures and techniques, and the interpretation of the observations and results.

Section 2

RESULTS

2.1 Experiments with Polystyrene Latex Microspheres

We have supported the design, performance, and analysis of a series of experiments on reactor performance. Thes experiments were done by Dale Kornfeld at MSFC. Our contributions included assisting in the improvement of the optical systems, and in setup and performance of the different tests.

The experiments were done with suspensions in water of monodisperse polystyrene latex microspheres, with diameters from 30 to 100 microns. The particle concentrations were of order 0.1% by volume. The reactor was a cylinder, with interior diameter 2.125 inches and length 3 inches. The curved boundary and one plane end boundary were transparent. The non-transparent end of the bath was a piston, moving in and out to compensate for changes in the fluid volume in the cylinder.

The reactor was set up with water, and allowed to reach uniform rotation. High-concentration latex suspension was then injected with a syringe through the moving piston. The syringe could be operated in and out with sufficient force to flush the syringe and to create turbulence inside the chamber, with thorough mixing. Within a minute of injection, observation showed uniform particle concentration, with no apparent deviations from solid body rotation of the fluid.

The particles were illuminated in a darkened laboratory by a vertical slice of laser light with thickness about a millimeter, entering horizontally and normal to the chamber axis. Refraction problems were minimized by filling the surrounding water bath. The particles in the illuminated slice could be viewed directly through the sides of the cylinder, and through a rotoscope at the end of the cylinder (which eliminated the rotation and made the chamber appear stationary). The light was strongest at small scattering angles from the incident light. The most useful results were obtained using a video camera, with a special cylindrical lens to make the image of the illuminated slice appear circular even though it was viewed at a small scattering angle. This led to focusing problems; our only solution to date has been to use so much light that the camera aperture was very small.

Until now, all our experiments have been done with latex particles of density 1.05, heavier than the fluid which was water. We are considering using the same latex particles in a fluid with a density greater than 1.05.

The first group of experiments were designed to confirm the rate of centrifugal spiralling outward, and therefore used relatively large rotation rates, of order 20rpm. At these rates, no secondary flow effects were observed. The exponential decrease in the particle concentration with time was measured, and was in agreement with the centrifugal settling theory.

The second group of experiments used lower rotation rates, from about 0.6rpm to 2rpm. At these rates, the centrifugal spiralling outward is relatively minor, and the depleted crescent formation is in theory likely to be more significant. This was confirmed, with a visible crescent on the descending side at 1.5rpm.

But at lower rotation rates, strong secondary flow effects became apparent, with time and space variations in the particle concentration and motion. The change with decreasing rotation rate was quite abrupt, especially at our largest concentration of 0.3%. At 1.5rpm nothing interesting happened except for the crescent, while at 0.7rpm the secondary flows grew rapidly, in about 10 minutes, and moved most of the particles to the walls, leaving thin plumes of high concentration ascending at the ascending wall, and descending across the chamber interior under their own weight. The patterns varied on a time scale of about 2 minutes. Large regions of the visible slice became almost void of particles. The results at 1rpm showed significant secondary flows, but they were not nearly so chaotic as those at 0.7rpm.

The flow fields were three-dimensional; this is the only explanation for some abrupt changes in the local concentration which were not advected in from adjacent parts of the visible slice. And they were driven by variations in the particle concentration.

2.2 Theory of the Secondary Flows

We have analyzed the video results extensively. Particles with specific density 1.05, at 0.3% concentration by volume, increase the density of the water by about 0.015%. Even at particle concentrations as low as 0.03%, the nonuniformities in the particle concentration clearly drive a secondary flow, superposed on the uniform rotation, for rotation rates of 1rpm and smaller. The nonuniformities in the particle concentration can arise only from the wall, since particle concentration is conserved following a fluid element, while decreasing exponentially at a low rate due to centrifugal buoyancy.

From observation, once particles collide with the wall (or with the aggregate of particles against the wall), only a small proportion are ever resuspended. The secondary flows are driven primarily by the net buoyancy of the depleted crescent, and secondarily by nonuniformities in the particle concentration associated with resuspension. Theoretically, these flows are proportional to the square of the thickness of the depleted crescent, which is in turn inversely proportional to the rotation rate. If these secondary flows become comparable with the solid body rotation, the theory based on uniform rotation breaks down completely, and the flows and particle distributions are quite different (and plainly three-dimensional in the videos).

The experiments make it plain that the lower limit on the rotation rate, predicted in the earlier theory based on the approximation of solid-body rotation, is not realistic for a concentration by volume of even 0.01%. But concentrations of up to 30% are used in typical recipes for polymerization of monomer-swollen latex microspheres. The rotation rate must be larger by a factor of order 100, so that the depletion layer thickness is only 1% of the diameter.

This statement assumes that the reactor has a length comparable with its diameter. If the length is very small compared with the diameter, then the secondary flows will be limited by viscous interaction with the ends.

In a latex reaction, the initial monomer-swollen particles have a relative density of order 0.9, and tend to centrifuge inwards, away from the walls. They increase in density as the absorbed low-density monomer is polymerized to high-density polymer, according to a non-linear conversion versus time curve. This buoyancy distribution will also establish its own secondary flow, and the overall result is hard to predict.

2.3 Computer Solution for Uniform Rotation

We have completed the computer program upgrade.

We reviewed two computer programs written by others. The first, FAST.FOR, was written by a summer student employee under the supervision of William Fowlis, during 1987. It implements the analysis of our report, and for given keyboard input parameters computes the various resulting parameters as described in the report. It also writes output files in a suitable form for the commercial EnerGraphics program, which reads these files and produces screen and printer plots of the spiral particle tracks.

The second program was written by John Cleland, at the Research Triangle Institute, NC. It is identified as KORN2.FOR, named for Dale Kornfeld, who manages this effort at MSFC. This program is a similar implementation of the analysis of our report, reading input parameters from the keyboard, and computing the various resulting parameters. It also generates simple plots of particles distributed at the computed concentration, at successive times, using the commercial Grapher software.

We chose to upgrade the second computer program and to add superior graphics. Basically, the two codes perform similar functions. The spiral plots produced by FAST.FOR are not particularly helpful, since in practical cases the thickness of the lines fills the figure. Similarly, it takes two of the KORN2.FOR particle plots to reveal a single concentration change factor. And the use of the EnerGraphics and Grapher packages, in two stages, was unnecessarily complex.

We corrected two errors in the KORN2.FOR program. First, there was a minor error in the computation of the viscosity of water at low temperatures, possibly caused by an error in transmission of the code. This is documented in Appendix A. Secondly, the approximate solution of a cubic equation for the parameter as a function of was seriously in error for larger values. We implemented a high-accuracy iterative solution, as described in Appendix B.

We upgraded the data input for the program. It now reads its parameters from a file containing the values used last, and the user need only enter changes from these values. Each program execution will compute cases one after the other, until the series is terminated by entering a negative time. Also, we implemented a variable reactor radius.

We have added optional graphic plots of the results. These graphics are plotted using the commercial software package GraphiC, from Scientific Endeavors Corporation, of Kingston, TN. For each case, two plots can be produced.

The first graphic is illustrated in Figure 1. It displays a cross section of the rotating reactor, with the fluid in solid-body rotation about the center O. There are two other concentric circles, centered on the point A where a stationary particle is just supported against its weight (net of the weight of the displaced fluid) by the viscous drag of the fluid flow past it. The interpretation of this figure is different depending on whether the particles are heavier or lighter than the fluid.

For particles heavier than the fluid, the fluid flow is counterclockwise in the figure, and is assumed to be solid-body rotation as described earlier. Particles at the point A remain stationary; with the downward force of gravity balanced by the upward buoyancy and drag forces. All other particles move outward from A in counterclockwise spiral orbits, with the radius increasing by a fixed and very small fraction on each orbit.

Particles which start in the crescent shape hit the lower semicircle of the wall during their first orbit. Ideally they can fall off the wall in the upper right of the figure, but observation of latex particle experiments suggests that few do, and the crescent is cleared of particles in ten or so rotations.

Heavy particles starting out between the two concentric circles spiral outwards during the fixed time period of interest until they cross the outer circle and hit the wall. As stated earlier, after one or more such impacts, they adhere to the wall, and do not fall away.

Heavy particles starting out inside the inner circle also spiral outwards, until at the end of the time of interest they fill the outer of the concentric circles. The particle concentration remains uniform during this process.

For particles lighter than the fluid, the fluid flow is clockwise in the figure, and is assumed to be solid-body rotation as described earlier. Particles at the point A remain stationary; with the upward buoyancy force due to the weight of the fluid displaced balanced by the downward gravity and drag forces. All other particles move inwards towards A in clockwise spiral orbits, with the radius decreasing by a fixed and very small fraction on each orbit.

Buoyant particles which start in the crescent shape hit the upper semicircle of the wall during their first orbit. In theory they can lift off the wall in the lower right of the figure, but the observations of latex particle experiments (with heavy particles, as described above) suggest that most of them will adhere to the wall, with the crescent cleared of particles in ten or fewer rotations.

Light particles starting out with uniform concentration inside the outermost of the two concentric circles spiral inwards during the fixed time period of interest. By the end of the time interval, they are all inside the inner circle, with their concentration still uniform.

The second graphic produced for each case is illustrated in Figure 2. It shows plots of the following three dimensionless functions of the rotation rate Ω (in rpm):

$$r_o/b = 1-\Omega_{min}/\Omega = 1-\delta;$$

$$r_i/r_o = \exp[-(\Omega/\Omega_{max})^2] = \exp(-\epsilon) \text{ ; and}$$

$$r_i/b = (1-\Omega_{min}/\Omega) \exp[-(\Omega/\Omega_{max})^2] = (1-\delta) \exp(-\epsilon) = \sqrt{F}.$$

Here r_i and r_o are the radii of the inner and outer concentric circles, and b is the reactor radius. The other notation is as in the report in Appendix D. We have chosen to maximize F, which is the ratio of the area of the small circle to the cross section area of the reactor. Thus the optimum rotation rate Ω corresponds to the peak value of the third function. It should be noted that the shape of the first two functions is always the same, but the form of their product depends on the relative values of Ω_{min} and Ω_{max}.

2.4 Report on Uniform-Rotation Theory

We have made changes to our earlier report "Particle Orbits in a Rotating Liquid" on rotating reactor theory, as requested by the referees, and resubmitted it to the Journal of Fluid Mechanics. The report is attached as Appendix D. This paper assumes solid-body fluid rotation, and neglects all secondary flows. It is the basis for the computer program described above.

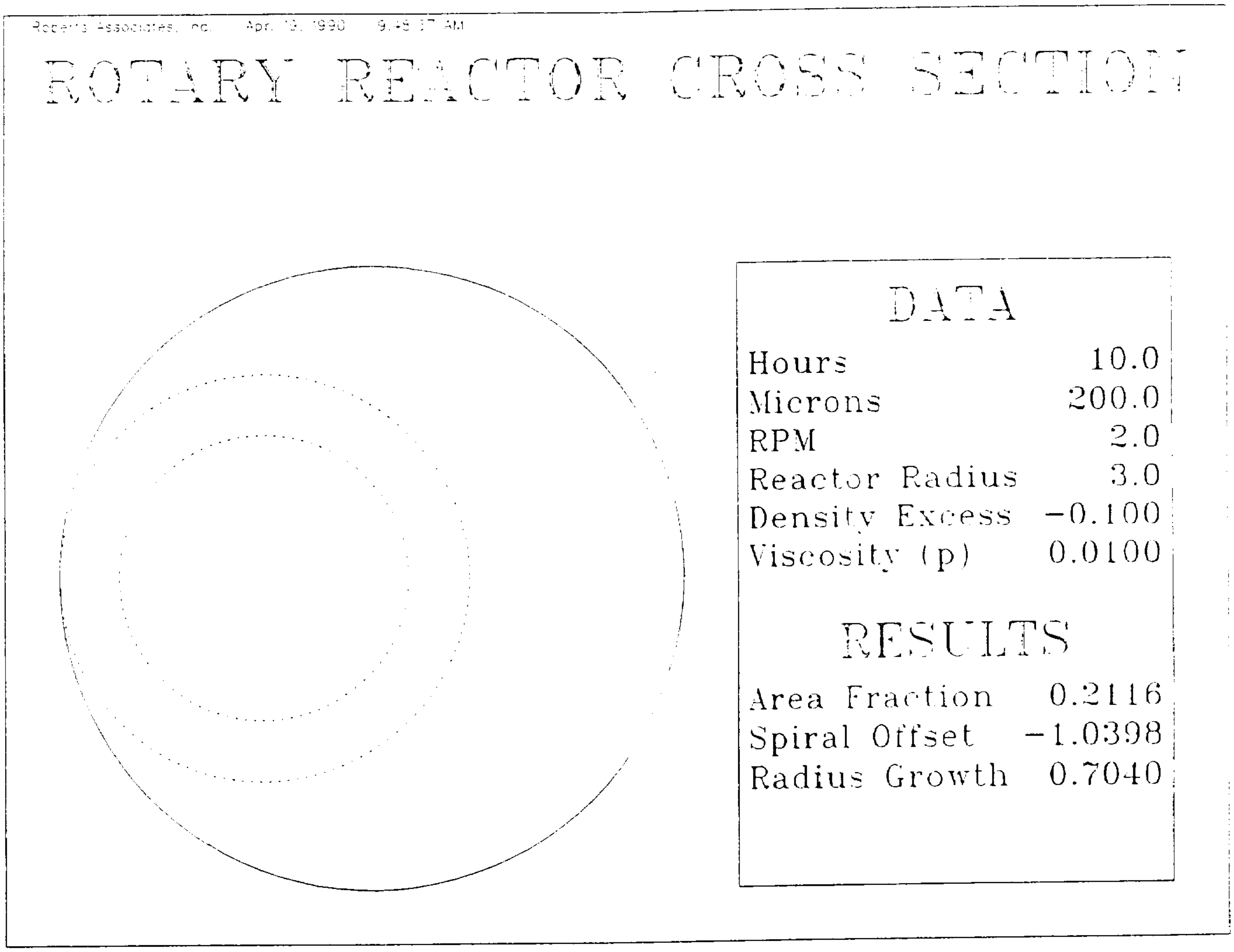

Figure 1. Reactor Cross Section with the Inner and Outer Circles

Particles starting in the crescent hit the wall immediately.
Heavy particles starting between the circles spiral out to hit the wall.
Heavy particles starting in the inner circle spiral out to fill the outer.
Light particles starting in the outer circle spiral in to fill the inner.

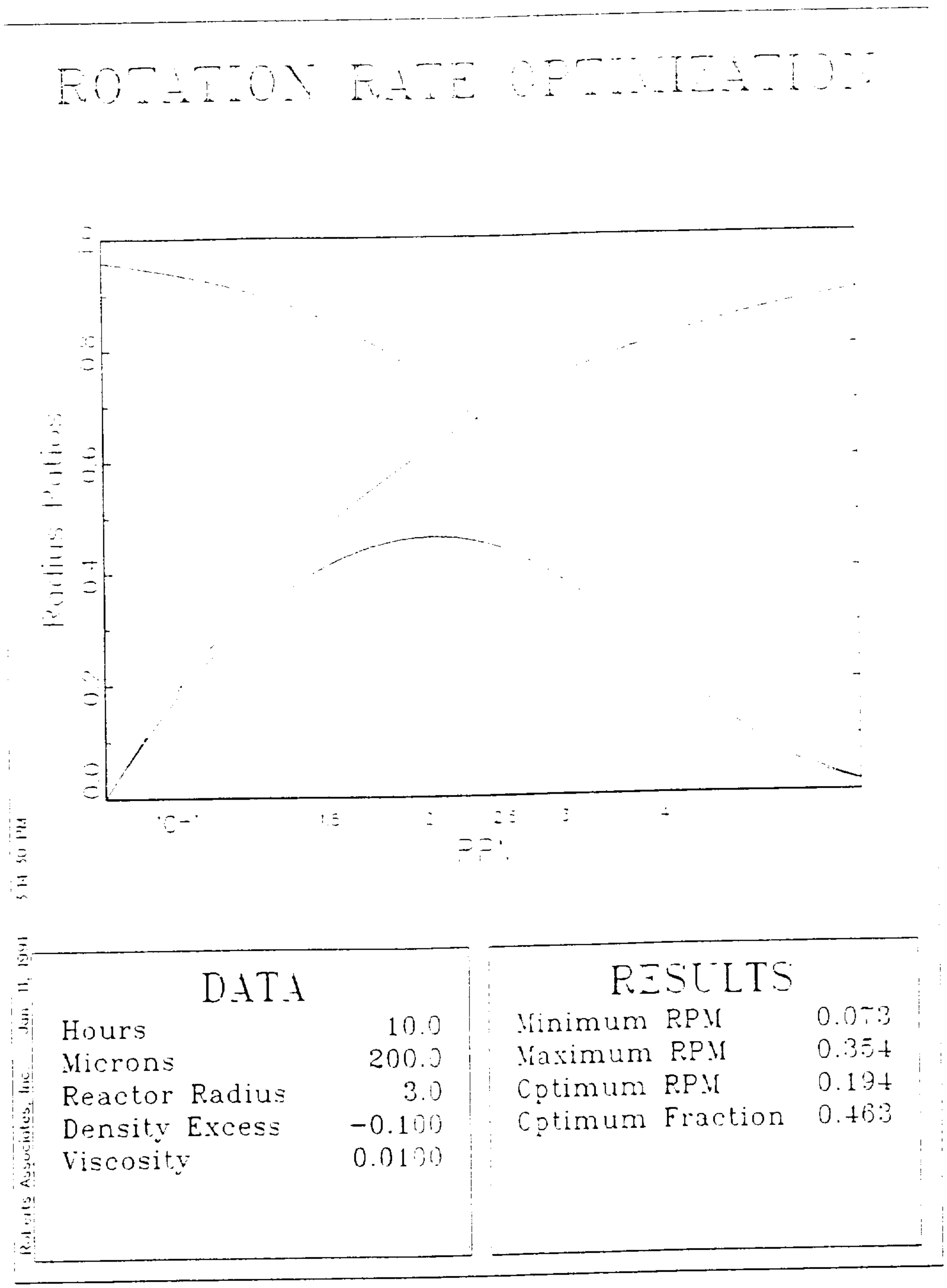

Figure 2. Sample Plot for Radius Ratios as Functions of Rotation Rate

Section 3

RECOMMENDATIONS

We strongly recommend an experimental investigation of reactor performance with intermediate concentrations of buoyant particles. It is likely that secondary flows will play a more important role in this case, because the depleted zone extends all round the boundary, and its thickness increases with time as the particles centrifuge inwards.

We recommend expanded analytic and numerical studies of the flows driven by thin depleted layers. We believe that an approximate analytic solution can be obtained using the methods of Ekman layer analysis, including end effects at the cylinder ends. These solutions can be confirmed and refined numerically, and with appropriate measurements. Such a program would provide a basis for optimizing the rotating reactor system and extending its range of application.

ACKNOWLEDGEMENTS

Dale Kornfeld of MSFC introduced me to this field, and was responsible for the experimental program which we supported. David Donovan of RAI has made significant contributions on the experimental side. I was privileged to work with William Fowlis of MSFC for many years before his deteriorating health and untimely death at the beginning of this year; we cooperated on this problem for several months. John Cleland, of Research Triangle Institute, NC, has provided helpful insights, and authored a computer program which was developed into the program described above.

<u>REFERENCES</u>

G. O. Roberts, W. W. Fowlis, and D. Kornfeld (1989); "Particle Orbits in a Rotating Liquid"; submitted to Journal of Fluid Mechanics.

G. O. Roberts (1984); "Models of Electroosmosis in Segmented Cylinders and the Effects of Rotation"; Report RAI-84-A-1, Roberts Associates, Incorporated, prepared for the University of Arizona.

G. O. Roberts, W. W. Fowlis, and T. L. Miller (1985); "The AGCE Code: Finite-Difference Fluid Dynamics Computer Mathematical Models for the Design and Interpretation of Experiments for Space Flight"; NASA Technical Paper 2323.

G. K. Batchelor and R. W. Janse Van Renburg (1986), "Structure Formation in Bidisperse Sedimentation"; J. Fluid Mech. <u>166</u>, 379-407.

Weast, ed., "Handbook of Physics and Chemistry", CRC Press, 70th Edition, 1989.

APPENDIX A

VISCOSITY FORMULATION FOR WATER

The viscosity of water decreases by a factor of 6 as the temperature increases from freezing to boiling. This change is important, as some processes of biological interest are done at low temperatures, while the production of monodisperse latex microspheres requires temperatures of order 70 degrees C.

Our computer program reads the temperature from the keyboard, and computes the viscosity using two empirical formulas from Weast (1989), based on data from the National Bureau of Standards. The formulas apply to temperature above and below 20 degrees C, and were included in the program KORN2.FOR which we have upgraded.

In validating the formulas, we discovered an error in their code implementation for low temperatures. The following program and listing computes the bad formula and the two good ones over the whole range of temperatures, and lists also the tabulated values from Weast (1989).

The following two points should be noted. First, the computed viscosity was too large by only about 1% at zero degrees, an insignificant error. Secondly, the formulas agree with the tabulated values for temperatures below and above 20 degrees, except that the tabulated values were truncated to four significant figures above 20 degrees, instead of being rounded.

NBSVISC.FOR Friday, January 11, 1991 3:50 pm Page 1

```
      program nbsvisc
c
c     NATIONAL BUREAU OF STDS. FORMULAE FOR H2O VISCOSITY (POISE,
c     OR 1 GM/SEC CM); CRC HANDBOOK OF CHEM. AND PHYS., 58TH ED.,
c     PP. F-49 TO F-51.
c

      write(0,2)
2     format(' COMPARISON OF NBS FORMULAS FOR VISCOSITY OF WATER'//
     1T3,'TEMP',T13,'VISCO',T25,'VISC1',T37,'VISC2',T46,'VISC1-VISC2'/)
      do 1 temp=0.,100.,2.

c             if (temp.le.20.) then
                    v=(1301./(998.333+8.1855*(temp-20.)+0.00585*
     1            ((temp-20.)*2))) - 3.30233
                    visc0=(10.0)**v
c
c     PROGRAM KORN2.FOR AS RECEIVED DID NOT SQUARE THE SECOND TERM
c     IN THE POWER SERIES
c
                    v=(1301./(998.333+8.1855*(temp-20.)+0.00585*
     1            ((temp-20.)**2))) - 3.30233
                    visc1=(10.0)**v
c             else
                    v=(1.3272*(20.-temp)-0.001053*((temp-20.)**2))/
     1            (temp+105.)
                    visc2=.01002 * (10.0)**v
c             endif

1     write(0,'(f8.0,4f12.8)') temp,visc0,visc1,visc2,visc1-visc2

      end
```

COMPARISON OF NBS FORMULAS FOR VISCOSITY OF WATER

TEMP	VISC0	VISC1	VISC2	VISC1-VISC2	TABLE IN EDITION 70, PAGE F-40
0.	.01806736	.01786897	.01776873	.00010024	1787
2.	.01685966	.01671371	.01663208	.00008163	
4.	.01577390	.01566859	.01560318	.00006541	
6.	.01479456	.01472047	.01466908	.00005138	
8.	.01390846	.01385806	.01381871	.00003935	
10.	.01310437	.01307162	.01304250	.00002912	1307
12.	.01237263	.01235273	.01233220	.00002053	
14.	.01170497	.01169405	.01168064	.00001340	
16.	.01109422	.01108921	.01108161	.00000760	
18.	.01053416	.01053263	.01052965	.00000298	
20.	.01001941	.01001941	.01002000	-.00000059	1002
22.	.00954526	.00954526	.00954847	-.00000321	
24.	.00910757	.00910637	.00911137	-.00000500	
26.	.00870273	.00869940	.00870544	-.00000604	
28.	.00832754	.00832136	.00832778	-.00000642	
30.	.00797920	.00796963	.00797584	-.00000622	7975
32.	.00765520	.00764184	.00764733	-.00000549	
34.	.00735334	.00733590	.00734020	-.00000431	
36.	.00707162	.00704992	.00705264	-.00000272	
38.	.00680831	.00678223	.00678300	-.00000077	
40.	.00656182	.00653130	.00652981	.00000149	6529
42.	.00633075	.00629578	.00629176	.00000402	
44.	.00611383	.00607444	.00606764	.00000680	
46.	.00590991	.00586617	.00585638	.00000979	
48.	.00571797	.00566995	.00565699	.00001296	
50.	.00553708	.00548488	.00546860	.00001629	5468
52.	.00536640	.00531013	.00529039	.00001974	
54.	.00520516	.00514495	.00512163	.00002332	
56.	.00505267	.00498865	.00496165	.00002700	
58.	.00490830	.00484060	.00480984	.00003076	
60.	.00477148	.00470023	.00466564	.00003459	4665
62.	.00464167	.00456702	.00452854	.00003848	
64.	.00451840	.00444048	.00439807	.00004241	
66.	.00440123	.00432016	.00427379	.00004638	
68.	.00428975	.00420568	.00415531	.00005037	
70.	.00418359	.00409665	.00404227	.00005438	4042
72.	.00408241	.00399272	.00393432	.00005841	
74.	.00398590	.00389359	.00383115	.00006244	
76.	.00389377	.00379895	.00373248	.00006647	
78.	.00380574	.00370854	.00363805	.00007050	
80.	.00372158	.00362211	.00354759	.00007451	
82.	.00364105	.00353941	.00346089	.00007852	
84.	.00356394	.00346024	.00337773	.00008251	
86.	.00349006	.00338439	.00329791	.00008648	
88.	.00341922	.00331168	.00322125	.00009043	
90.	.00335124	.00324193	.00314758	.00009435	
92.	.00328598	.00317498	.00307674	.00009825	
94.	.00322329	.00311069	.00300857	.00010212	
96.	.00316302	.00304890	.00294294	.00010596	
98.	.00310506	.00298949	.00287972	.00010977	
100.	.00304927	.00293233	.00281878	.00011355	

VISC0 USES THE BAD T<20 FORMULA IN MY COPY OF KORN2.FOR (OMITTED * IN (T-20)**2). THIS MAY HAVE BEEN A TRANSMISSION ERROR.

VISC1 IS CORRECTED, AND AGREES WITH THE 4 SIGNIFCANT FIGURES IN THE REFERENCE.

VISC2 (FOR T>20) AGREES WITH THE REFERENCE, EXCEPT THAT THE REFERENCE TABLE VALUES ARE TRUNCATED TO 4 FIGURES INSTEAD OF ROUNDED!

APPENDIX B

SOLUTION OF THE CUBIC EQUATION FOR DELTA

The two programs FAST.FOR and KORN2.FOR made available to us for upgrade did not attempt to solve a cubic equation for δ as a function of Φ, which arises in our analysis in the report in Appendix A of the optimization of the rotation rate. Physically and mathematically, δ increases from zero to one as Φ increases from zero to infinity. The second program introduced three approximate formulations for δ, nominally valid in different ranges of Φ. We have replaced these with an efficient iterative solution. The following program validates our solution algorithm, and compares it with the approximations.

The program takes a representative set of exact δ values, and for each one it computes the corresponding ϕ. Without using the known δ, it computes the three empirical approximations and the first five iterations. The results list the exact value, the empirical approximations, their errors, the ϕ value, the fifth iteration value, and the errors of the first five iterative values.

The following points should be noted. First, the empirical formulas are reasonable for ϕ values up to about 1.3, with errors in δ of less than 10%. Secondly, the first formula is better than the second for δ values up to 0.15, rather than the 0.05 in the supplied code. Thirdly, the empirical formula is a disaster for larger ϕ values, predicting an unphysical δ value of more than unity, and leading to program failure when a fractional power of $1-\delta$ is evaluated.

COMPARISON OF CLELAND "CURVE FITTING" SOLUTIONS FOR DELTA WITH EXACT VALUE AND SIMPLE NEWTON ITERATION SOLUTION

DEL	DELC1	DELC2	DELC3	DIF1	DIF2	DIF3	PHI	DELI5	DIFI1	DIFI2	DIFI3	DIFI4	DIFI5
.00000	.00000	.00000	.00000	.00000	.00000	.00000	.00000	.00000	0.0E-00	0.0E-00	0.0E-00	0.0E+00	0.0E-00
.01000	.01003	.00923	.01246	.00003	-.00077	.00246	.01003	.01000	-2.3E-10	6.9E-17	-4.2E-17	-4.2E-17	-4.2E-17
.02000	.02014	.01843	.02286	.00014	-.00157	.00286	.02014	.02000	-4.4E-09	6.6E-17	-4.5E-17	-4.5E-17	-4.5E-17
.03000	.03031	.02767	.03263	.00031	-.00233	.00263	.03031	.03000	-2.3E-08	-5.5E-16	1.1E-16	-3.5E-18	-3.5E-18
.04000	.04055	.03694	.04205	.00055	-.00306	.00205	.04055	.04000	-7.1E-08	-5.2E-15	4.2E-17	4.2E-17	4.2E-17
.05000	.05086	.04626	.05122	.00086	-.00374	.00122	.05086	.05000	-1.7E-07	-3.1E-14	-1.4E-17	-1.4E-17	-1.4E-17
.06000	.06125	.05564	.06022	.00125	-.00436	.00022	.06125	.06000	-3.6E-07	-1.3E-13	8.3E-17	-2.3E-17	-2.3E-17
.07000	.07171	.06507	.06909	.00171	-.00493	-.00091	.07171	.07000	-6.7E-07	-4.3E-13	-2.3E-17	-2.3E-17	-2.3E-17
.08000	.08225	.07457	.07785	.00225	-.00543	-.00215	.08225	.08000	-1.1E-06	-1.3E-12	8.3E-17	-2.3E-17	-2.3E-17
.09000	.09287	.08412	.08653	.00287	-.00588	-.00347	.09287	.09000	-1.8E-06	-3.4E-12	8.3E-17	-2.3E-17	-2.3E-17
.10000	.10357	.09374	.09515	.00357	-.00625	-.00485	.10357	.10000	-2.3E-06	-7.9E-12	-5.6E-17	-5.6E-17	-5.6E-17
.15000	.15835	.14290	.13771	.00835	-.00710	-.01229	.15835	.15000	-1.4E-05	-2.1E-10	-5.6E-17	-5.6E-17	-5.6E-17
.20000	.21544	.19400	.18006	.01544	-.00600	-.01994	.21544	.20000	-4.4E-05	-2.1E-09	5.6E-17	-5.6E-17	-5.6E-17
.25000	.27516	.24735	.22281	.02516	-.00265	-.02719	.27516	.25000	-1.1E-04	-1.2E-08	-8.3E-17	-8.3E-17	-8.3E-17
.30000	.33787	.30329	.26643	.03787	.00329	-.03357	.33787	.30000	-2.2E-04	-5.3E-08	-3.0E-15	-5.6E-17	-5.6E-17
.35000	.40405	.36224	.31133	.05405	.01224	-.03867	.40405	.35000	-4.0E-04	-1.3E-07	-3.5E-14	-1.1E-16	5.6E-17
.40000	.47425	.42470	.35794	.07425	.02470	-.04206	.47425	.40000	-6.3E-04	-5.1E-07	-2.9E-13	0.0E+00	0.0E+00
.45000	.54924	.49135	.40675	.09924	.04135	-.04325	.54924	.45000	-1.1E-03	-1.3E-06	-1.9E-12	-5.6E-17	-5.6E-17
.50000	.62996	.56302	.45834	.12996	.06302	-.04166	.62996	.50000	-1.6E-03	-2.9E-06	-9.7E-12	-5.6E-17	-5.6E-17
.55000	.71773	.64088	.51347	.16773	.09088	-.03653	.71773	.55000	-2.2E-03	-5.9E-06	-4.2E-11	1.1E-16	0.0E+00
.60000	.81433	.72649	.57315	.21433	.12649	-.02685	.81433	.60000	-3.0E-03	-1.1E-05	-1.5E-10	-1.1E-16	0.0E+00
.65000	.92234	.82214	.63881	.27234	.17214	-.01119	.92234	.65000	-4.0E-03	-2.0E-05	-4.9E-10	-1.1E-16	0.0E+00
.70000	1.04566	.93125	.71257	.34566	.23125	.01257	1.04566	.70000	-5.0E-03	-3.2E-05	-1.3E-09	-1.1E-16	-1.1E-16
.75000	1.19055	1.05932	.79782	.44055	.30932	.04782	1.19055	.75000	-6.1E-03	-4.3E-05	-3.1E-09	0.0E+00	0.0E+00
.80000	1.36798	1.21601	.90041	.56798	.41601	.10041	1.36798	.80000	-7.0E-03	-6.6E-05	-6.1E-09	0.0E+00	0.0E+00
.85000	1.59976	1.42049	1.03189	.74976	.57049	.18189	1.59976	.85000	-7.6E-03	-8.0E-05	-9.2E-09	-1.1E-16	0.0E+00
.90000	1.93899	1.71939	1.22001	1.03899	.81939	.32001	1.93899	.90000	-7.3E-03	-7.7E-05	-8.3E-09	-1.1E-16	0.0E+00
.91000	2.03061	1.80006	1.27006	1.12061	.89006	.36006	2.03061	.91000	-7.0E-03	-7.3E-05	-8.0E-09	-1.1E-16	0.0E+00
.92000	2.13513	1.89204	1.32680	1.21513	.97204	.40680	2.13513	.92000	-6.7E-03	-6.7E-05	-6.9E-09	-1.1E-16	0.0E+00
.93000	2.25658	1.99889	1.39229	1.32658	1.06889	.46229	2.25658	.93000	-6.3E-03	-6.0E-05	-5.5E-09	0.0E+00	0.0E+00
.94000	2.40110	2.12599	1.46962	1.46110	1.18599	.52962	2.40110	.94000	-5.8E-03	-5.1E-05	-4.1E-09	0.0E+00	0.0E+00
.95000	2.57870	2.28210	1.56384	1.62870	1.33210	.61384	2.57870	.95000	-5.2E-03	-4.1E-05	-2.7E-09	0.0E+00	0.0E+00
.96000	2.80706	2.48272	1.68376	1.84706	1.52272	.72376	2.80706	.96000	-4.5E-03	-3.1E-05	-1.5E-09	0.0E+00	0.0E+00
.97000	3.12175	2.75900	1.84700	2.15175	1.78900	.87700	3.12175	.97000	-3.5E-03	-2.0E-05	-6.2E-10	0.0E+00	0.0E+00
.98000	3.61035	3.18758	2.09632	2.63035	2.20758	1.11632	3.61035	.98000	-2.5E-03	-9.5E-06	-1.5E-10	0.0E+00	0.0E+00
.99000	4.59517	4.05025	2.58629	3.60517	3.06025	1.59629	4.59517	.99000	-1.2E-03	-2.3E-06	-8.7E-12	0.0E+00	0.0E+00
.99100	4.76423	4.19820	2.66895	3.77323	3.20720	1.67795	4.76423	.99100	-1.1E-03	-1.8E-06	-5.5E-12	0.0E+00	0.0E+00
.99200	4.96000	4.36948	2.76420	3.96800	3.37748	1.77220	4.96000	.99200	-9.3E-04	-1.4E-06	-3.2E-12	0.0E+00	0.0E+00
.99300	5.19099	4.57151	2.87597	4.19799	3.57851	1.88297	5.19099	.99300	-8.0E-04	-1.0E-06	-1.8E-12	0.0E+00	0.0E+00
.99400	5.47019	4.81563	3.01021	4.47619	3.82163	2.01621	5.47019	.99400	-6.7E-04	-7.2E-07	-8.7E-13	0.0E+00	0.0E+00
.99500	5.81880	5.12031	3.17659	4.82380	4.12531	2.18159	5.81880	.99500	-5.4E-04	-4.7E-07	-3.7E-13	0.0E+00	0.0E+00
.99600	6.27441	5.51832	3.39211	5.27841	4.52232	2.39611	6.27441	.99600	-4.1E-04	-2.7E-07	-1.2E-13	0.0E+00	0.0E+00
.99700	6.91281	6.07568	3.69076	5.91581	5.07868	2.69376	6.91281	.99700	-2.9E-04	-1.3E-07	-3.0E-14	0.0E+00	0.0E+00
.99800	7.92113	6.95527	4.15535	6.92313	5.95727	3.15735	7.92113	.99800	-1.7E-04	-4.3E-08	-3.9E-15	0.0E+00	0.0E+00
.99900	9.99000	8.75766	5.08588	8.99100	7.75866	4.08688	9.99000	.99900	-6.9E-05	-7.9E-09	-1.1E-16	0.0E+00	0.0E+00
.99910	10.34812	9.06937	5.24428	9.34902	8.07027	4.24518	10.34812	.99910	-6.0E-05	-6.0E-09	-1.1E-16	0.0E+00	0.0E+00
.99920	10.76356	9.43087	5.42714	9.76436	8.43167	4.42794	10.76356	.99920	-5.1E-05	-4.4E-09	0.0E+00	0.0E+00	0.0E+00
.99930	11.25460	9.85804	5.64212	10.25530	8.85874	4.64282	11.25460	.99930	-4.3E-05	-3.0E-09	0.0E+00	0.0E+00	0.0E+00
.99940	11.84920	10.37512	5.90082	10.84980	9.37572	4.90142	11.84920	.99940	-3.5E-05	-2.0E-09	0.0E+00	0.0E+00	0.0E+00
.99950	12.59291	11.02163	6.22206	11.59341	10.02213	5.22256	12.59291	.99950	-2.7E-05	-1.2E-09	0.0E+00	0.0E+00	0.0E+00
.99960	13.56666	11.86770	6.63898	12.56706	10.86810	5.63938	13.56666	.99960	-2.0E-05	-6.7E-10	0.0E+00	0.0E+00	0.0E+00
.99970	14.93353	13.05463	7.21780	13.93383	12.05493	6.21810	14.93353	.99970	-1.4E-05	-3.0E-10	0.0E+00	0.0E+00	0.0E+00
.99980	17.09634	14.93120	8.12000	16.09654	13.93140	7.12020	17.09634	.99980	-7.8E-06	-9.9E-11	0.0E+00	0.0E+00	0.0E+00
.99990	21.54219	18.78364	9.93054	20.54229	17.78374	8.93064	21.54219	.99990	-3.0E-06	-1.4E-11	0.0E+00	0.0E+00	0.0E+00

EXACT SOLUTION — CLELAND SOLUTIONS WITH SOLUTION APPLICABLE TO THIS PHI VALUE MARKED. — DIFFERENCES BETWEEN CLELAND AND EXACT SOLUTIONS — PHI — 5TH ITERATION — ERRORS FOR FIRST THRU 5TH ITERATIONS

NOTE THAT THE FIRST ITERATION IS VERY GOOD, AND THE THIRD IS EFFECTIVELY EXACT. THE CALCULATION USED DOUBLE PRECISION.

NOTE THAT DEL VALUES OVER UNITY ARE UNPHYSICAL.
PARAMETERS LEADING TO PHI VALUES OVER 1.6 CAUSE KORN2.EXE TO FAIL.

```
      PROGRAM SOLVCUBC
      IMPLICIT REAL*8 (A-H,O-Z)

10    FORMAT(' COMPARISON OF CLELAND "CURVE FITTING" SOLUTIONS '
     1 ,'FOR DELTA WITH EXACT'
     2 ,' VALUE AND SIMPLE NEWTON ITERATION SOLUTION'//
     3 ,14A9/)

      WRITE(0,10)'DEL','DELC1','DELC2','DELC3','DIF1','DIF2','DIF3'
     1        ,'PHI','DELI5','DIFI1','DIFI2','DIFI3','DIFI4','DIFI5'

C SELECT A RANGE OF EXACT DEL VALUES BETWEEN ZERO AND ONE

      DO IDEL=0,90,10
      DEL=IDEL/1000.D0
      CALL SOLVE(DEL)
      ENDDO

      DO IDEL=100,850,50
      DEL=IDEL/1000.D0
      CALL SOLVE(DEL)
      ENDDO

      DO IDEL=900,990,10
      DEL=IDEL/1000.D0
      CALL SOLVE(DEL)
      ENDDO

      DO IDEL=991,999,1
      DEL=IDEL/1000.D0
      CALL SOLVE(DEL)
      ENDDO

      DO IDEL=9991,9999,1
      DEL=IDEL/10000.D0
      CALL SOLVE(DEL)
      ENDDO

      END


      SUBROUTINE SOLVE(DEL)
      IMPLICIT REAL*8 (A-H,O-Z)

      DIMENSION DIFF(5)

      THIRD=1/3.D0

      PHI=DEL/(1-DEL)**THIRD

C THE PROBLEM IS TO SOLVE THIS EQUATION FOR DEL, WITH PHI KNOWN,
C (WITHOUT USING THE KNOWN DEL VALUE, OF COURSE).

C CLELAND "CURVE-FITTING" SOLUTIONS APPLY TO DIFFERENT PHI REGIONS
C AS INDICATED BY THE COMMENTS

c            if (PHI .le. .05) then
                   DELC1=PHI
c            else
                   DELC2=.89086*PHI**.99301
c                  if (DELC2.gt.0.60) then
                          DELC3 = .6854*PHI**0.8708
c                  endif
```

```
c               endif

C NEWTON'S ITERATION SOLUTION

C INITIAL APPROXIMATION IS EXACT SOLUTION OF THE EQUATION
C WITH THE CUBES REPLACED BY SQUARES

        PHI2=PHI*PHI
        DELI=(SQRT(PHI2*(4+PHI2))-PHI2)/2

C ITERATE
C R IS THE FIRST RESIDUAL FORMULATION, AND RD IS ITS DERIVATIVE
C USE S = 1-(1-R)**3, AND ITS DERIVATIVE SD, TO GIVE FASTER CONVERGENCE
C AND AVOID PROBLEMS FOR LARGE PHI.

        DO 2 I=1,5
        ROOT=(1-DELI)**THIRD
        R=DELI-PHI*ROOT
        RD=1+PHI*THIRD*ROOT/(1-DELI)
        T=1-R
        T2=T*T
        S=1-T2*T
        SD=3*T2*RD
        DELI=DELI-S/SD

C SAVE DIFFERENCE FROM EXACT SOLUTION, FOR DISPLAY

2       DIFF(I)=DELI-DEL

C WRITE OUT THE SOLUTIONS AND ERRORS

        write(0,'(9f9.5,1P,5E9.1)')DEL,DELC1,DELC2,DELC3
     1                        ,DELC1-DEL,DELC2-DEL,DELC3-DEL,PHI,DELI,DIFF

        end
```

APPENDIX C

THE ROTREAC COMPUTER PROGRAM

The source programs ROTREAC.FOR and CPLOT.C are listed on the following pages. The source programs, the executable ROTREAC.EXE (compiled and linked with Microsoft software), and the commercial package GraphiC (with a single user license) have been supplied to Robert S. Snyder and Dale Kornfeld of MSFC. The executable should not be distributed to any user without a GraphiC license. The executable ROTREACD.EXE was made using the replacement dummy program CPLOTD.C, and does not call the GraphiC package; RAI authorizes the general distribution of this code.

The program runs on IBM PC or AT compatibles, and can produce graphics on a very wide range of displays and printers. Before running the program for the first time, it is necessary to run the program EQUIP.EXE, which comes with the GraphiC software. This program allows the user to select a display option and printer options from a menu of choices, and writes a permanent configuration file which is read each time by the ROTREAC program. More details are of course provided with the software. The environment parameter GPC should be set to C:\GPC, or to some other DOS directory containing font files and the files written by EQUIP.EXE.

The program solicits keyboard input for each of eight parameters defining the problem. For each parameter, the default is the value used the last time, which is saved in the file ROTREAC.DAT and used if the input data is null. Once each case is finished, the program begins again, soliciting new keyboard data. The sequence of cases is terminated using Ctrl-Break (or any other interrupt such as invalid data, Ctrl-C, power off, or Alt-Ctrl-Del) at any stage, or by providing a negative time in response to the first prompt of a new case.

For each case, the program writes its output to the screen. After producing its text output for each case, the program produces graphs. These are written both to the screen and to the graphics file ROTREAC.TKF. Printer output is produced by responding to the beep prompt with the keys L or l (for large full-page plots at high or low resolution), or M or m (for medium half-page plots at high or low resolution).

Once the run is over, the graphics file can be played back using the command

PLAY ROTREAC.TKF

(where PLAY.EXE is another GraphiC program). This leads to the same beep prompts as the graphs are displayed, with the same printer options. There is little point in using this option, however, since the ROTREAC program runs quickly, and can be run again to obtain any desired graphical output. The full list of beep options is below.

Sample screen output (obtained using Ctrl-P) is also shown below. File output is similar, except that the prompts and data entry are not shown. Items after the colons are entered from the keyboard. The source programs are listed on the following pages.

```
The allowable choices are:
         c --> convert TKF file to another format
         l --> large, low resolution plot
         L --> large, high resolution plot
         m --> medium sized, low resolution plot
         M --> medium sized, high resolution plot
         p --> change printer selections
         q --> quit and close files
         v --> vary PostScript parameters
         w --> shrink picture to fit window
         z --> zoom marked area to fill screen
        CR --> go on to next plot
 space bar --> to return to picture
```

```
ENTER ANY CHANGES FROM THE BRACKETED DATA USED LAST.
ALWAYS INCLUDE THE DECIMAL POINT WHEN YOU ENTER DATA.
THEN PRESS THE ENTER KEY.
TOTAL TIME IN HOURS (NEGATIVE TO QUIT) [ 10.0000] :
 PARTICLE DIAMETER (MICRONS) [200.0000] :
 ROTATION RATE (RPM) [   2.0000] :
 REACTOR RADIUS (CM) [   3.0000] :
 PARTICLE DENSITY [   1.1000] :
 FLUID DENSITY [   1.2000] :
 TEMPERATURE (DEG c) [ 20.0000] :
 ALTERNATE VISCOSITY (POISE) (NEGATIVE MEANS USE WATER @ T) [    .0100] :
```

PROBLEM PARAMETERS:

TIME (HR)	PARTICLE DIAM(MICRON)	ROTATION RATE RPM	ROTATION RATE RAD/SEC	REACTOR RADIUS(CM)	DENSITIES PARTICLE	DENSITIES FLUID	VISCOSITY POISE
10.0	200.00	2.000	.2094	3.0000	1.1000	1.2000	.01000

SPIRAL ORBIT DESCRIPTION:

FINAL CONCENTRATION	AREA FRACTION	XOFFSET (CM)	BRADIUS (CM)	SRADIUS (CM)	REYNOLDS NUMBER	TAYLOR NUMBER	SPIRAL GROWTH PER RADIAN
2.01746	.21162	-1.0398	1.9602	1.3801	2.6E-01	2.5E-03	-4.7E-05

ROTATION RATE CHOICE:

OMAX 1/SEC	OMIN 1/SEC	PHI	DELTA	AREA FRACTION	ROTATION RATE 1/SEC	ROTATION RATE RPM
.354	.072593	.43850	.37493	.21447	.1936	1.8489

```
          INTERFACE TO SUBROUTINE BGNPLOT [C,ALIAS:'_bgnplot']
     x    (MP,ISC,TKFILE)
          INTEGER *2 MP,ISC
          CHARACTER *20 TKFILE [REFERENCE]
          END

          INTERFACE TO SUBROUTINE CPLOT [C] (TIMH,ADIAM,RPM,BRAD,DRHO,VISCOS
     1 ,ARERAT,XSPIRAL,BRADIUS,SRADIUS
     1 ,OMAX,OMIN,OMOPT,FOPT)
          REAL *4 TIMH,ADIAM,RPM,BRAD,DRHO,VISCOS
     x    ,ARERAT,XSPIRAL,BRADIUS,SRADIUS
     x     ,OMAX,OMIN,OMOPT,FOPT
          END

          INTERFACE TO SUBROUTINE STOPPLOT [C,ALIAS:'_stopplot'] ()
          END

          PROGRAM ROTREAC

C         ANALYZE ROTATING REACTOR PERFORMANCE
C         ASSUME FLUID REMAINS IN SOLID-BODY ROTATION

                  IMPLICIT REAL*4 (A-H,O-Z)

                  LOGICAL LEXIST

           MP = 1
           ISC = 'g'
           CALL BGNPLOT(MP,ISC,'ROTREAC.TKF'C)

C         GET INITIAL VALUES OF PARAMETERS FROM DATA FILE OR INITIAL DEFAULTS.
C         OPEN DATA FILE.

                  INQUIRE(FILE='ROTREAC.DAT',EXIST=LEXIST)

                  IF (.NOT. LEXIST) THEN
                          TIMH=20.
                          TEMP=20.
                          RHOP=1.05
                          RHOF=1.00
                          VALT=-1.
                          ADIAM=20
                          BRAD=3
                          RPM=1.
                          OPEN(1,FILE='ROTREAC.DAT',STATUS='NEW')
                  ELSE
                          OPEN(1,FILE='ROTREAC.DAT',STATUS='OLD')
                          READ(1,'(/8F10.5)')
     1            TIMH,TEMP,RHOP,RHOF,VALT,ADIAM,BRAD,RPM
                  ENDIF

C         READ IN CHANGES FROM DATA OF LAST RUN

C         FORMATS

 30               FORMAT(1X,A,F8.4,'] :'\)
 31               FORMAT(F10.3)
 32               FORMAT(/' ENTER ANY CHANGES FROM THE BRACKETED DATA USED LAST.'
     1    /' ALWAYS INCLUDE THE DECIMAL POINT WHEN YOU ENTER DATA.'
     1    /' THEN PRESS THE ENTER KEY.')

C         CONTROL RETURNS HERE FROM THE END OF THE PROGRAM

```

```
33          WRITE(0,32)

C     READ TIME IN HOURS, STOP ON NEGATIVE. CONVERT TO SECONDS

            WRITE(0,30) 'TOTAL TIME IN HOURS (NEGATIVE TO QUIT) [',TIMH
            READ (0,31) TIMHD
            IF (TIMHD .LT. 0.0) THEN
                    CALL STOPPLOT
                    STOP ' '
            ENDIF
            IF (TIMHD .NE. 0.0) TIMH = TIMHD
            TIMSEC=TIMH*3600.

C     READ IN PARTICLE DIAMETER IN MICRONS
C     COMPUTE THE PARTICLE RADIUS IN CM.

            WRITE(0,30) 'PARTICLE DIAMETER (MICRONS) [',ADIAM
            READ(0,31) ADIAMD
            IF (ADIAMD .GT. 0.0) ADIAM = ADIAMD
            ARAD=ADIAM*0.0001/2.

C     READ IN REACTOR ROTATION RATE IN RPM AND CONVERT TO RAD/SEC

            WRITE(0,30) 'ROTATION RATE (RPM) [',RPM
            READ(0,31) RPMD
            IF (RPMD .NE. 0.0) RPM = RPMD
            ONE=1
            PI=4*ATAN(ONE)
            OMEGA=RPM*2*PI/60

C     READ IN REACTOR REACTOR RADIUS (CM).

            WRITE(0,30) 'REACTOR RADIUS (CM) [',BRAD
            READ(0,31) BRADD
            IF (BRADD .GT. 0.0) BRAD = BRADD

C     READ IN SPECIFIC GRAVITY (DENSITY IN GM/CC) FOR THE FLUID
C     AND THE PARTICLES.

            WRITE(0,30) 'PARTICLE DENSITY [',RHOP
            READ(0,31) RHOPD
            IF (RHOPD .GT. 0.0) RHOP = RHOPD

            WRITE(0,30) 'FLUID DENSITY [',RHOF
            READ(0,31) RHOFD
            IF (RHOFD .GT. 0.0) RHOF = RHOFD

C     READ IN REACTOR WATER TEMPERATURE IN DEGREES CENTIGRADE (FOR VISCOSITY)

            WRITE(0,30) 'TEMPERATURE (DEG c) [',TEMP
            READ(0,31) TEMPD
            IF (TEMPD .GT. 0.0) TEMP = TEMPD

C     NATIONAL BUREAU OF STDS. FORMULAE FOR WATER VISCOSITY ( POISE,
C     OR 1 GM/SEC CM); CRC HANDBOOK OF CHEM. AND PHYS., 70TH ED., p. F-40.

            IF (TEMP.LE.20.) THEN
                    V=(1301./(998.333+8.1855*(TEMP-20.)+0.00585*
     1       ((TEMP-20.)**2))) - 3.30233
                    VISCOS=(10.0)**V
            ELSE
                    V=(1.3272*(20.-TEMP)-0.001053*((TEMP-20.)**2))/
     1       (TEMP+105.)
```

```
                     VISCOS=.01002 * (10.0)**V
                ENDIF

C       PUT IN ALTERNATE VISCOSITY IN POISE IF DESIRED (AND IGNORE TEMPERATURE)

                WRITE(0,30)
     1'ALTERNATE VISCOSITY (POISE) (NEGATIVE MEANS USE WATER @ T) ['
     2,VALT
                READ(0,31) VALTD
                IF (VALTD .NE. 0.0) VALT = VALTD
                IF (VALT  .GT. 0.0) VISCOS = VALT

C       WRITE OUT DATA (DEFAULTS FOR NEXT RUN)

                REWIND 1
                WRITE(1,'(8A10/8F10.5)')
     1  'TIMH','TEMP','RHOP','RHOF','VALT','ADIAM','BRAD','RPM'
     1  ,TIMH , TEMP , RHOP , RHOF , VALT , ADIAM , BRAD , RPM
                REWIND 1

C       SPECIFY THE MEAN EARTH GRAVITATIONAL CONSTANT (980 G/CM**2).

C       COMPUTE THE DRAG CONSTANT, CDRAG (1/SEC) WHICH IS THE RATE AT
C       WHICH MOTION DECAYS THROUGH DRAG FORCES ALONE. IT IS ONLY
C       USED MULTIPLIED BY RHOP; THE PRODUCT IS CALLED CDR.

C       COMPUTE THE OFFSET OF THE SPIRAL CENTER, XSPIRAL (CM) FROM
C       THE REACTOR CENTER, ALONG THE X AXIS.

C       COMPUTE THE CENTRIFUGAL GROWTH RATE D (1/SEC) FOR THE SPIRAL RADIUS.

C       THE FINAL RADIAL DISPLACEMENT FROM THE SPIRAL CENTER OF ANY
C       PARTICLE IS DELR TIMES THE INITIAL RADIAL DISPLACEMENT.
C       THE PARTICLE CONCENTRATION STAYS UNIFORM, AND IS MULTIPLIED
C       BY CONC.

                G=980.

                CDR=9.*VISCOS/(2.*ARAD**2)
                CDRAG=CDR/RHOP

                DRHO=(RHOP-RHOF)
                ADELRH=ABS(DRHO)

                XSPIRAL=(G*DRHO)/(OMEGA*CDR)
                AXSP=ABS(XSPIRAL)

                D=(DRHO*OMEGA**2)/CDR

                ETA = D*TIMSEC
                AETA = ABS(ETA)
                DELR=EXP(ETA)
                CONC=1 / (DELR*DELR)

C       COMPUTE THE REYNOLDS AND TAYLOR DIMENSIONLESS PARAMETERS.
C       BOTH SHOULD BE MUCH LESS THAN UNITY FOR A VALID SOLUTION.
C       THE RATIO D/OMEGA (SPIRAL GROWTH PER RADIAN) MUST ALSO BE
C       SMALL FOR A VALID SOLUTION.

                REY = RHOF*ARAD*AXSP*OMEGA/VISCOS
                TAYLOR = RHOF*ARAD**2*OMEGA/VISCOS
                SPGRPR = D/OMEGA

```

```
C       COMPUTE THE RADIUS RSPIRAL (cm) OF THE SMALL CIRCLE.

C       HEAVY PARTICLES ORIGINALLY IN THE CIRCLE DO NOT SPIRAL OUT TO
C       HIT THE WALL IN TIME TIMH.

C       BUOYANT PARTICLES WHICH DO NOT HIT THE WALL DURING THE FIRST
C       SPIRAL SPIRAL INWARDS TO INSIDE THIS CIRCLE IN TIME TIMH.

              DELTA = AXSP/BRAD
              BRADIUS = BRAD-AXSP
              SRADIUS = BRADIUS*EXP(-AETA)
              ARERAT = (SRADIUS/BRAD)**2

C       THE REMAINING CALCULATIONS IGNORE THE GIVEN ROTATION RATE

C       COMPUTE THE MAXIMUM AND MINIMUM VALUES OF THE ROTATION RATE (RAD/SEC).

C       THE MINIMUM IS DEFINED SO THAT THE SPIRAL CENTER IS AT THE REACTOR RADIUS
C       THE MAXIMUM IS DEFINED ARBITRARILY BY ABS(ETA)=1, SO THAT PARTICLES
C       MIGRATE INWARDS OR OUTWARDS CENTRIFUGALLY BY A FACTOR e IN TIME TIMH.

              OMAX = (CDR/(ADELRH*TIMSEC))**0.5
              OMIN = G*(ADELRH)/(BRAD*CDR)

C       AN OPTIMIZED ROTATION RATE IS COMPUTED BY MAXIMIZING THE RATIO OF THE
C       AREA INSIDE THE SPIRAL RADIUS TO THE REACTOR AREA.
C       FIRST DEFINE PHI. NOTE THAT PHI**3/2 = (OMMIN/OMMAX)**2 = (ARAD/AMAX)**6

              THIRD=1/3.D0

              PHI = (2.*ARAD**6*G**2*TIMSEC/BRAD**2)**THIRD
     1        *(2.*ADELRH/(9.*VISCOS))

C       SOLVE DEL = PHI*(1-DEL)**(1/3)
C       DEL IS OMOPT/OMMIN = XSPIRAL/BRAD

C       NEWTON'S ITERATION SOLUTION

C       INITIAL APPROXIMATION IS EXACT SOLUTION OF THE EQUATION
C       WITH THE CUBE ROOT REPLACED BY A SQUARE ROOT. THE POSITIVE
C       ROOT IS CHOSEN, AND FORMULATED TO AVOID ROUNDING ERROR FOR
C       VERY LARGE PHI

              PHI2=PHI*PHI
              DELI=PHI2*2/(SQRT(PHI2*(4+PHI2))+PHI2)

C       ITERATE
C       R IS THE FIRST RESIDUAL FORMULATION, AND RD IS ITS DERIVATIVE
C       USE S = 1-(1-R)**3, AND ITS DERIVATIVE SD, TO GIVE FASTER CONVERGENCE
C       AND AVOID PROBLEMS FOR LARGE PHI.

              DO 2 I=1,5
              ROOT=(1-DELI)**THIRD
              R=DELI-PHI*ROOT
              RD=1+PHI*ROOT*THIRD/(1-DELI)
              Q=1-R
              Q2=Q*Q
              S=1-Q2*Q
              SD=3*Q2*RD
    2         DELI=DELI-S/SD

              DELOPT=DELI
              FOPT = (1-DELOPT)**2/EXP(PHI**3/DELOPT**2)
```

```
            OMOPT = (G/(2.*BRAD*TIMSEC*(1-DELOPT)))**THIRD

C      AN APPROXIMATE UPPER LIMIT ON PARTICLE RADIUS, AMAX (CM), IS COMPUTED
C      BY EQUATING OMAX AND OMIN. ALL OTHER CALCULATIONS USE THE GIVEN SIZE.

            AMAX = (9.*VISCOS/(2.*ADELRH))**0.5*
     1      (BRAD**2/(G**2*TIMSEC))**(1./6.)
            DMAX = AMAX*20000.

            WRITE(0,80)TIMH,ADIAM,RPM,OMEGA,BRAD,RHOP,RHOF,VISCOS

            IF (BRAD.GT.ABS(XSPIRAL)) THEN
                  WRITE(0,81)CONC,ARERAT,XSPIRAL,BRADIUS,SRADIUS,REY,TAYLOR,SPGRPR
            ELSE
                  WRITE(0,83)CONC,ARERAT,XSPIRAL,BRADIUS,SRADIUS,REY,TAYLOR,SPGRPR
            ENDIF

            WRITE(0,82)OMAX,OMIN,PHI,DELOPT,FOPT,OMOPT,OMOPT*30/PI

 80    FORMAT(//' PROBLEM PARAMETERS:',/,
     1 '  TIME     PARTICLE    ROTATION RATE    ',
     1 ' REACTOR      DENSITIES     VISCOSITY',/,
     2 '  (HR)   DIAM(MICRON)  RPM    RAD/SEC    ',
     2 'RADIUS(CM) PARTICLE FLUID    POISE',/,
     3 F6.1,F12.2,F10.3,F8.4,F12.4,F9.4,F8.4,F9.5,//)

 81    FORMAT(' SPIRAL ORBIT DESCRIPTION:',/,
     1 '      FINAL        AREA    XOFFSET  BRADIUS SRADIUS ',
     1 'REYNOLDS  TAYLOR  SPIRAL GROWTH',/,
     2 ' CONCENTRATION FRACTION    (CM)     (CM)     (CM)    ',
     3 ' NUMBER    NUMBER     PER RADIAN',/,
     4 F10.5,F12.5,F8.4,F9.4,F8.4,1P,2E9.1,E11.1//)

 83    FORMAT(' SPIRAL ORBIT DESCRIPTION IMPOSSIBLE:',/,
     1 '      FINAL        AREA    XOFFSET  BRADIUS SRADIUS ',
     1 'REYNOLDS  TAYLOR  SPIRAL GROWTH',/,
     2 ' CONCENTRATION FRACTION    (CM)     (CM)     (CM)    ',
     3 ' NUMBER    NUMBER     PER RADIAN',/,
     4 F10.5,F12.5,F8.4,F9.4,F8.4,1P,2E9.1,E11.1//)

 82    FORMAT(' ROTATION RATE CHOICE:',/,
     1 '  OMAX     OMIN      PHI     DELTA     AREA      ',
     1 'ROTATION RATE ',/,
     3 '   1/SEC     1/SEC                    FRACTION    ',
     1 '1/SEC      RPM  ',/,
     5 F7.3,F9.6,3F9.5,2F9.4,//)

      WRITE (0,*) 'ENTER N IF YOU DO NOT WANT A PLOT'
      READ (0,'(A1)') CNO
      IF (CNO.EQ.'N') GO TO 33

        CALL CPLOT (TIMH,ADIAM,RPM,BRAD,DRHO,VISCOS
     1 ,ARERAT,XSPIRAL,BRADIUS,SRADIUS
     1 ,OMAX,OMIN,OMOPT,FOPT)

        GO TO 33

C       IT KEEPS SOLICITING A NEW CASE, AND STOPS ON A NEGATIVE TIMH VALUE

        END
```

```
#include "graphic.h"            /* Will include all necessary include files */

/*
      CALL CPLOT (TIMH,ADIAM,RPM,BRAD,DRHO,VISCOS,ARERAT
     1 ,XSPIRAL,BRADIUS,SRADIUS
     1 ,OMAX,OMIN,OMOPT,FOPT)
*/

void cplot (float timn, float adiam, float rpm, float brad, float drho, float viscos,
                              float arerat, float xspiral, float bradius, float sradius,
                              float omax, float omin, float omopt, float fopt )
{

/*
   declarations
*/
        float brads,xs,bra,sra,rgrowth;
        int i,nxdiv,nydiv,npts;
        char buffer[99];
        float om[301], y[301], z[301], w[301];
        float ymin, ymax, ystep, omaxd;

/*
   first plot
*/
   if (abs(xspiral)<brad)
        {
                /* CONVERT TO RADIUS 2.3 INCHES */
                xs=(2.3/brad)*xspiral;
                bra=(2.3/brad)*bradius;
                sra=(2.3/brad)*sradius;
                brads=2.3;
                startplot(7);    /* initializes each plot and sets the background color */
                   /* 0-7 are black, blue, green, cyan; red, magenta, brown, white */
                font(3,"simplex.fnt",'\310',"triplex.fnt",'\311',"complex.fnt",'\312'
                        ,"",' ');
                                                  /* loads your chosen fonts */
                rotate(0);
                page(9.,6.855);                     /* sets the output page size */
                setscale(0);
                              /* this is the same aspect ratio as 4095 by 3119 */
                /* cross(1);                          crossed axes if either axis goes through zero */
                /* area2d(8.0,5.5);           sets the area of the plot (drawing page) */
                color(2);                              /* Green */
                box();
                color(5);                              /* sets color to magenta */
                tmargin(.15);
                ctline("\311ROTARY REACTOR CROSS SECTION",.31);   /* titles plot */
                color(4);                              /* sets color to red */
                dashf(1);
                circle(2.7+0.,2.7+0.,brads,0.,6.3);
                dashf(9);
                circle(2.7+xs,2.7+0.,bra,0.,6.3);
                circle(2.7+xs,2.7+0.,sra,0.,6.3);
                color(2);                              /* Green */
                dateit('\310');

                page(3.2,4.6);
                pgshift(5.4,.4);
                linesp(1.8);
                setscale(1);
                box();

```

```
        lmargin(.2);

        tmargin(.0);
        ctline("\311DATA",.7);

        tmargin(1.5);
        sprintf(buffer,"%8.1f",timh);
        rtline(buffer,.45);
        sprintf(buffer,"%8.1f",adiam);
        rtline(buffer,.45);
        sprintf(buffer,"%8.1f",rpm);
        rtline(buffer,.45);
        sprintf(buffer,"%8.1f",brad);
        rtline(buffer,.45);
        sprintf(buffer,"%8.3f",drho);
        rtline(buffer,.45);
        sprintf(buffer,"%8.4f",viscos);
        rtline(buffer,.45);

        tmargin(1.5);
        ltline("Hours",.45);
        ltline("Microns",.45);
        ltline("RPM",.45);
        ltline("Reactor Radius",.45);
        ltline("Density Excess",.45);
        ltline("Viscosity",.45);

        tmargin(7.0);
        ctline("\311RESULTS",.7);

        tmargin(8.5);
        sprintf(buffer,"%8.4f",arerat);
        rtline(buffer,.45);
        sprintf(buffer,"%8.4f",xspiral);
        rtline(buffer,.45);
        if (drho>0.) rgrowth=bradius/sradius;
        else                     rgrowth=sradius/bradius;
        sprintf(buffer,"%8.4f",rgrowth);
        rtline(buffer,.45);

        tmargin(8.5);
        ltline("Area Fraction",.45);
        ltline("Spiral Offset",.45);
        ltline("Radius Growth",.45);

        endplot();
}
/* END OF IF BLOCK ON XSPIRAL TEST. START OPTIMIZATION PLOT */

startplot(7);    /* initializes each plot and sets the background color */
   /* 0-7 are black, blue, green, cyan; red, magenta, brown, white */
font(3,"simplex.fnt",'\310',"triplex.fnt",'\311',"complex.fnt",'\312'
        ,"",' ');
                                        /* loads your chosen fonts */
rotate(90);
page(6.855,9.);                         /* sets the output page size */
setscale(0);
                  /* this is the same aspect ratio as 4095 by 3119 */
color(2);                                 /* Green */
box();
color(5);                                 /* sets color to magenta */
tmargin(.12);
ctline("\311ROTATION RATE OPTIMIZATION",.25);   /* titles plot */
```

```
        color(4);                                    /* sets color to red */
        dateit('\310');
        ymin=0.;
        ymax=1;
        ystep=.2;
        page(6.855,5.5);                             /* sets the output page size */
        pgshift(0.,2.7);
        area2d(5.855,4.0);                                  /* Plot diminisions */
        color(10);                                              /* Black grid */
        grid(1);                                            /* Dotted line grid */
        fgrid(2,2,2);                 /* Subdivide the plot with tick marks only */
        frame(1,1);                            /* Draw a frame around the plot */
        cross(0);                                           /* Do not cross axes */
        fntchg('\310');                        /* Change fonts for axes labels */
omaxd=max(2*omax,5*omin);
        for(i=0; i<=300; i++){                           /* Make vectors to plot */
                om[i]=omin*exp(log(omaxd/omin)*i/300.);
                y[i]=1-omin/om[i];
                z[i]=exp(-(om[i]/omax)*(om[i]/omax));
    w[i]=y[i]*z[i];
        }
        npts=301;                                /* Size of the x & y vectors */
        xlog(omin,omaxd,"%-1.1f",ymin,ystep,ymax);     /* Manual scaled om-axis */
        color(11);
        xname("\310RPM");                                      /* om-axis name */
        yname("\310Radius Ratios");                              /* Y-axis name */
        color(10);
        curve(om, y, npts, 0);                  /* Draw curve with no symbols */
        color(14);
        curve(om, z, npts, 0);                             /* Draw second curve */
        color(12);
        curve(om, w, npts, 0);                             /* Draw  third curve */

        page(3.2,2.2);
        pgshift(.15,.15);
        linesp(1.8);
        box();

        lmargin(.2);
        tmargin(.0);
        ctline("\311DATA",.20);

        tmargin(.38);
        sprintf(buffer,"%8.1f",timh);
        rtline(buffer,.13);
        sprintf(buffer,"%8.1f",adiam);
        rtline(buffer,.13);
        sprintf(buffer,"%8.1f",brad);
        rtline(buffer,.13);
        sprintf(buffer,"%8.3f",drho);
        rtline(buffer,.13);
        sprintf(buffer,"%8.4f",viscos);
        rtline(buffer,.13);

        tmargin(.38);
        ltline("Hours",.13);
        ltline("Microns",.13);
        ltline("Reactor Radius",.13);
        ltline("Density Excess",.13);
        ltline("Viscosity",.13);

        page(3.2,2.2);
        pgshift(3.5,.15);
```

CPLOT.C Friday, January 11, 1991 4:24 pm Page 4

```
        box();

        lmargin(.2);
        tmargin(.0);
        ctline("\311RESULTS",.20);

        tmargin(.38);
        sprintf(buffer,"%8.3f",omin);
        rtline(buffer,.13);
        sprintf(buffer,"%8.3f",omax);
        rtline(buffer,.13);
        sprintf(buffer,"%8.3f",omopt);
        rtline(buffer,.13);
        sprintf(buffer,"%8.3f",sqrt(fopt));
        rtline(buffer,.13);

        tmargin(.38);
        ltline("Minimum RPM",.13);
        ltline("Maximum RPM",.13);
        ltline("Optimum RPM",.13);
        ltline("Optimum Fraction",.13);

        endplot();
        scrt(); /* text mode for interactive stuff */
}
```

CPLOTD.C Friday, January 11, 1991 4:25 pm Page 1

```
void cplot (float timh, float adiam, float rpm, float brad, float drho, float viscos,
                                float arerat, float xspiral, float bradius, float sradius,
                                float omax, float omin, float omopt, float fopt )
{
}
void bgnplot (int mp, int isc, char * tkfile)
{
}

void stopplot ()
{
}
```

APPENDIX D

PARTICLE ORBITS IN A ROTATING LIQUID

An earlier version of the appended report, with William Fowlis as the first author, was submitted in early 1988 to Prof. Owen Phillips at Johns Hopkins University, for publication in the Journal of Fluid Mechanics. A favorable report was received from the two referees, with only minor corrections required. Submission of a corrected version was delayed by the increasing incapacity of Dr. Fowlis, who went on extended sick leave in the summer of 1988, later took medical disability retirement, and died at the beginning of 1989.

With the concurrence of Dale Kornfeld and of Dr. Robert S. Snyder (supervisor of Dr. Fowlis at MSFC until his retirement) Dr. Roberts of RAI agreed to become first author and to resubmit the paper. The new version follows.

Roberts Associates, Incorporated
380 West Maple Avenue, Suite L-1A
Vienna, VA 22180-5616

(703)242-2115 or (703)356-5630
(Washington Metropolitan Area)

January 10, 1991

Prof. O.M. Phillips
Journal of Fluid Mechanics
Dept. of Earth and Planetary Sciences
The Johns Hopkins University
Baltimore, MD 21218

Dear Professor Phillips:

I enclose a revised manuscript for our paper "Particle Orbits in a Rotating Liquid". I believe this revision satisfies all the comments both of referees A and B.

Bill Fowlis died in December, 1988. He had been increasingly sick for three years, with what was ultimately diagnosed as a form of Parkinson's disease. He stopped working in the summer of 1988.

Dale Kornfeld and Dr. Robert S. Snyder (of Code ES76, MSFC, Tel. 205/544-7818 and 7805) have agreed that I should be identified as first author, as reflected on the amended title page. Dr. Snyder is the contracting officer's technical representative on my company's contracts, and is Kornfeld's supervisor. He was also Bill Fowlis's supervisor until his death.

The original manuscript was lost from the word-processor. You will note that this manuscript is a photocopy, with the changes cut-and-pasted in. I hope this is acceptable; it was easier than retyping the whole thing would have been. I do not have originals for the figures 1 and 2; so if you do mot have them, please let me know and we will get replacements to you.

I believe this revision satisfies all the comments and suggestions of referees A and B.

We have included the references mentioned by referee A, and one other new reference. Also, we have corrected the Ekman number definition; we thank him for pointing out this error.

With regard to the first paragraph of referee B, our process has been used to make large spherical latex microspheres with quality and uniformity approaching that of microgravity processing, as described in Section 1, at the bottom of page 3. And our analysis has been used in setting the rotation rate range for new rotating apparatus designs; we have expanded Section 5 slightly to clarify this.

We have modified the paper in response to suggestions 2 and 3 of referee B. With regard to suggestion 1, equations (27) through (29) are derived from equation (16), using the approximation (24), as stated at the bottom of page 11.

Suggestion 4 is answered by the whole of Section 4, where a specific optimization problem is solved. We have modified the text on page 15 to emphasize that this is done without using (33). A slightly different optimization problem might have a slightly different answer for the optimum rotation rate. There is no strict upper limit on the rotation rate; but the faster the chamber spins, the more rapidly the particles centrifuge outward to the walls or inward towards the axis.

We have added Figure 3, to clarify the optimization problem solved in Section 4. And we have added brief remarks on page 25 concerning secondary flows driven by the excess density distribution due to variations in the particle concentration.

We thank the referees for their work.

I apologize for the delay in returning this paper. This should have been done much more quickly after Bill's death.

Yours sincerely,

Dr. Glyn O. Roberts
President

PARTICLE ORBITS IN A ROTATING LIQUID

by

Glyn O. Roberts

Roberts Associates, Incorporated
380 West Maple Avenue, Suite L-1A
Vienna, VA 22180-5616

and

Dale M. Kornfeld

and

William W. Fowlis[1]

Space Science Laboratory, Code ES76
NASA Marshall Space Flight Center
Huntsville, Alabama 35812

[1] Dr. Fowlis died in December, 1988

Abstract

Monodisperse latex microspheres ranging in size from submicrometer to several micrometers in diameter can be prepared in the laboratory. The uniformity of diameter is important for instrument calibration and other applications. However it has proved very difficult to manufacture commercial quantities of monodisperse latex microspheres with diameters larger than about 3 micrometers due to buoyancy and sedimentation effects. In an attempt to eliminate these effects NASA sponsored a Space Shuttle experiment called the Monodisperse Latex Reactor (MLR) to produce these monodisperse microspheres in larger sizes in microgravity. Results have been highly successful.

Using technology gained from this space experiment, a ground-based rotating latex reactor has been fabricated in an attempt to minimize sedimentation without using microgravity. The entire reactor cylinder is rotated about a horizontal axis to keep the particles in suspension.

Abstract (continued)

In this paper we determine the motion of small spherical particles under gravity, in a viscous fluid rotating uniformly about a horizontal axis. The particle orbits are approximately circles, with centers displaced horizontally from the axis of rotation. Due to net centrifugal buoyancy, the radius of the circles increases (for heavy particles) or decreases (for light particles) with time, so that the particles gradually spiral inward or outward.

For a large rotation rate, the particles spiral outwards or inwards too fast, while for a small rotation rate, the displacement of the orbit center from the rotation axis is excessive in relation to the reactor radius. We determine the rotation rate which maximizes the fraction of the reactor cross section area which contains particles which will not spiral out to the wall in the experimental time (for heavy particles), or which have spiralled in without hitting the wall (for light particles). Typically, the rate is close to 1 rpm, and design rotation rate ranges should span this value.

1. INTRODUCTION

There is a need for microscopic spherical particles of an extremely uniform (monodisperse) size. These particles, called microspheres, are used as calibration standards for optical and electron microscopes, and for many other scientific purposes. Since 1947 monodisperse polystyrene latexes have been widely used for these applications.[1]

These early particles ranged in size from submicrometer to several micrometers (μm) in diameter. Over the years as larger polystyrene microspheres were prepared, a major difficulty in their manufacture was that amounts of coagulum produced always increased along with size, giving complete coagulum instead of particles in the size range greater than about 10 μm. Attempts to adjust the chemistry of the latex to reduce coagulum usually resulted in the production of a non-monodisperse latex, contaminated with particles of other sizes.[2]

The main cause of these problems was buoyancy and sedimentation effects. During the early stages of a seeded emulsion polymerization reaction using standard techniques and equipment, the large monomer-swollen latex seed particles tend to rise to the surface of the mixture (cream) because the average density of the particles is less than that of the water medium in which they are suspended. During the later stages of the polymerization, the growing seed particles become heavier as more lower-density monomer is converted to higher-density polymer, and they settle to the bottom of the reactor. As the particles are grown to sizes larger than about 2 μm (at which size they show only little Brownian motion) the rates of creaming and settling become so rapid that it is not possible to keep the particles in suspension using conventional paddle or propeller-type stirrers without resorting to excessive agitation rates. The growing particles are soft and sticky, and increasing the stirring rate causes more violent particle-particle collisions, resulting in flocculation. Since agitating the particles at rates high enough to prevent creaming or settling also results in flocculation, a different method of agitation had to be developed to produce these larger-size monodisperse latex particles. Another possible solution was to put the particles in an environment in which no stirring was needed at all.

Because this difficulty in producing usable quantities of monodisperse polystyrene latex particles in sizes greater than about 3 µm is gravity related, NASA sponsored a research effort to determine whether or not it would be possible to manufacture them in the microgravity environment of space.

This effort resulted in the highly successful Monodisperse Latex Reactor (MLR) Space Processing Experiment, which has now been flown into Earth orbit on five space shuttle missions. With Dr. John W. Vanderhoff of Lehigh University as the principal investigator, this MLR experiment has successfully produced large-particle monodisperse polystyrene latexes up to 30 µm in diameter with coefficients of variation of less than 2 percent.[3]

The 10 µm and 30 µm microspheres manufactured aboard the Space Shuttle are currently being marketed by the U. S. National Bureau of Standards as Standard Reference Material (SRM) #1960 and SRM #1961 respectively. These are the first products ever manufactured in space to be commercially marketed on Earth.[4,5]

During the course of the space experiments, one of the authors (D.M.K. - who is also NASA Co-Investigator with Dr. Vanderhoff on the MLR experiment) proposed that, as part of the supporting ground-based research, the same seeded emulsion polymerization recipes currently being used in space also be tested in a laboratory rotating-cylinder reactor. He then designed and fabricated a prototype Rotary Reactor (Figure 1) to minimize gravitational settling on Earth for the growing latex particles.

In this apparatus a cylindrical polymerization reactor chamber is rotated about its horizontal axis within a water bath. The Rotary Reactor is designed to maintain uniformity in particle concentration and temperature profile with minimal or no stirring. The particles are kept in suspension only through the rotation of the reactor, the slow rotation of the entire chamber during polymerization helps to prevent the growing particles from either creaming or settling. Once steady rotation of the seed latex mixture is achieved in this apparatus, there is no agitation to cause the violent particle collisions that result in flocculation.

It has already been established experimentally that large-size latex particles up to 100 μm diameter can be successfully suspended and polymerized at low reactor rotation rates. Particles manufactured thus far in this prototype reactor have exhibited coefficients of variation inferior to those produced in

ORIGINAL PAGE IS
OF POOR QUALITY

the Space Shuttle, but it is expected that latex quality will improve as latex recipes are optimized for this type reactor and optimum rotation rates are determined for each particle size and latex recipe.

As mentioned earlier, the density of the seed latex particles increases with time, through the conversion of the low density styrene monomer into the higher density polystyrene polymer, so the growing particles undergo a constant increase in density throughout the course of the reaction. While slowly rotating in this manner the particles are strongly influenced by viscous drag and tend to rotate with the fluid medium. Their motion relative to the rotating fluid is determined by a balance of their gravitational and centrifugal forces with the viscous drag, and the sign of the buoyancy forces depends on the density difference between the particles and the fluid.

At higher rotation rates, more dense particles will tend to be centrifuged outward and deposited on the cylinder wall of the Rotary Reactor. Less dense particles will be centrifuged inwards and will form a mass near the axis. A lower limit on the rotation rate is determined by the time it takes the particles to fall through (or rise through) a distance close to the radius of the reactor cylinder. Clearly there is an optimization problem for the rotation rate.

In this paper the particle orbits in the Rotary Reactor are determined, and the optimization problem is solved with the assumption that the particle density and radius remain fixed. Section 2 contains the formulation and solution of the particle orbit problem and Section 3 contains the formulation and solution of the rotation rate optimization problem. In Section 3 the principal conclusions are stated.

2. FORMULATION AND SOLUTION OF THE PROBLEM FOR PARTICLE ORBITS

Basic mechanisms for the suspension of heavy particles in a rotating cylinder of fluid were discussed by Otto and Lorenz[6], but a formal solution was not obtained. A more complete study of the particle orbit problem was presented by Schatz,[7] but the centrifugal buoyancy was not handled correctly. Related studies by Dill and Brenner[8], by Nadim, Cox and Brenner[9], by Aoki, Shirane, Tokimoto and Nakagawi[10], and by Annamalai and Cole[11], addressed parts of the problem. In their later work, Annamalai and Cole[12] obtained an orbit solution essentially equivalent to ours, in the context of bubbles. None of these references analyzed the optimization problem studied here.

In this section the particle orbit problem is correctly solved. The ambient fluid is taken to be in solid-body rotation about the horizontal z axis through the origin (see Figure 2) with rotation rate Ω. Then the fluid flow in the (x,y) plane is given by

$$\underline{u} = \underline{\Omega} \times \underline{x} = (-\Omega y,\ \Omega x) \ . \tag{1}$$

The corresponding pressure distribution is

$$p = p_o + \rho_f\left(\frac{1}{2}\,\Omega^2 r^2 - gy\right) , \tag{2}$$

where p_o is a constant, ρ_f is the fluid density and r^2 is $x^2 + y^2$, so that r is the cylindrical radius coordinate. The gradient of this pressure balances the gravitational and centrifugal forces on the fluid.

The vector equation of motion for a spherical particle of radius a, density ρ_p, volume V, and mass M at position $\underline{x}$ is

$$M\ddot{\underline{x}} = -Mg\hat{\underline{y}} + \underline{P} + \underline{D} \quad , \tag{3}$$

where the stress forces exerted by the fluid on the particle have been separated into a pressure force $\underline{P}$ and a drag force $\underline{D}$.

The pressure force is defined as

$$\underline{P} = -\int p dS \quad , \tag{4}$$

where p is the fluid pressure given by equation (2) above, and the integration is over the particle surface. Using Gauss' theorem,

$$\underline{P} = \rho_f V(-\Omega^2 x,\ g-\Omega^2 y). \tag{5}$$

The g term is the familiar Archimedes buoyancy force. The Ω^2 term is the corresponding inward pressure gradient which would cancel the centrifugal acceleration of the liquid which the particle has displaced. This term was apparently omitted by Schatz[7].

The drag force is written using the Stokes slow-flow approximation. In this viscous limit

$$\underline{D} = -\ 6\pi\eta a(\dot{\underline{x}} - \underline{\Omega} \times \underline{x}) \tag{6}$$

where η is the fluid viscosity. The drag force opposes the motion of the particle relative to the fluid. The approximation requires that the Reynolds number and the Taylor number be much smaller than unity, where

$$Re = \rho_f aV/\eta , \tag{7}$$

$$Ta = \rho_f a^2 \Omega/\eta , \tag{8}$$

and V is the relative motion of the particle ($V = |\dot{\underline{x}} - \underline{\Omega} \times \underline{x}|$).

Combining these expressions, the two non-trivial components of the equation of motion can be written as

$$\ddot{x} + c\dot{x} + \frac{\rho_f}{\rho_p} \Omega^2 x + c\Omega y = 0 , \tag{9}$$

$$\ddot{y} + c\dot{y} + \frac{\rho_f}{\rho_p} \Omega^2 y - c\Omega x = - \frac{\Delta\rho}{\rho_p} g , \tag{10}$$

where the drag constant,

$$c = \frac{9\eta}{2\rho_p a^2} , \tag{11}$$

is the rate at which motion decays through drag forces alone and $\Delta\rho = \rho_p - \rho_f$. The term on the right hand side of equation (10) arises from the particle weight less the Archimedes buoyancy force. The Ω^2 terms on the left hand sides of the equations (9) and (10) arise from the centrifugal pressure term in equation (5).

The coupled x and y equations can be solved conveniently by introducing the complex variable

$$w = x + iy. \tag{12}$$

Multiplying equation (10) by i and adding equation (9) gives the complex, second-order, linear equation

$$\ddot{w} + c\dot{w} + \left(\frac{\rho_f}{\rho_p}\,\Omega^2 - ic\Omega\right)w = -\,i\,\frac{\Delta\rho}{\rho_p}\,g. \tag{13}$$

The general solution of equation (13) is the sum of a particular integral and a complementary function

$$w = w_o + A_1 \exp(m_1 t) + A_2 \exp(m_2 t). \tag{14}$$

For this problem the particular integral is the constant

$$w_o = x_o + iy_o = \frac{\Delta\rho g}{\rho_p c\Omega}\left(1 + i\,\frac{\rho_f}{\rho_p}\,\frac{\Omega}{c}\right)^{-1}. \tag{15}$$

The real and imaginary parts represent the equilibrium position of the particle in the x-y plane. The complex constants m_1 and m_2 are the roots of the quadratic auxiliary equation

$$m^2 + cm + \left(\frac{\rho_f}{\rho_p}\,\Omega^2 - ic\Omega\right) = 0. \tag{16}$$

The complex constants A_1 and A_2 are determined by the initial values $w(0)$ and $\dot{w}(0)$ at time zero, using the equations

$$A_1 + A_2 = w(0) - w_o\ , \tag{17}$$

$$m_1 A_1 + m_2 A_2 = \dot{w}(0). \tag{18}$$

These simultaneous equations can be easily solved for A_1 and A_2.

The general solution (14) represents the superposition of two spiral motions about the equilibrium position (x_o, y_o). Consider the one solution

$$w = x + iy = A_1 \exp(m_1 t) , \tag{19}$$

where

$$A_1 = \alpha \exp(i\theta) , \tag{20}$$

$$m_1 = m_r + im_i . \tag{21}$$

Here α is the positive amplitude of A_1 and θ is its phase, while m_r and m_i are the real and imaginary part of m_1. The real and imaginary parts of w are

$$x = \alpha\, e^{m_r t} \cos(m_i t + \theta) , \tag{22}$$

$$y = \alpha\, e^{m_r t} \sin(m_i t + \theta). \tag{23}$$

The instantaneous spiral radius is $\alpha\, e^{m_r t}$, and grows or decays exponentially depending on the sign of m_r. The phase angle $m_i t + \theta$ determines the direction of the vector displacement (x,y) in the x-y plane.

We now use the inequality

$$\Omega << c. \tag{24}$$

Note that for $\eta \sim 10^{-2}$ gm/cm sec, $\rho_p \sim 1$ gm/cc and $a \sim 10^{-3}$ cm (corresponding to a diameter of 20 μm), c is 4.5×10^4 sec^{-1}. Thus even for much larger radii, this assumption is valid for a very wide range of practical rotation rates.

Using this approximation, the spiral center (15) is at

$$w_o = x_o + iy_o = \frac{g\Delta\rho}{\Omega c\rho_p} = \frac{2ga^2\Delta\rho}{9\eta\Omega} , \tag{25}$$

so that the spirals are centered about a point on the x-axis, displaced horizontally from the axis of rotation. At this point the drag force balances the net weight. Naturally, this point must be inside the rotating reactor, since if the point is outside or on the rotating reactor wall all the particle orbits will strike the wall. This puts a lower limit on Ω ;

$$\Omega > \Omega_{min} = \frac{g|\Delta\rho|}{bc\rho_p} = \frac{2ga^2|\Delta\rho|}{9\eta b} , \tag{26}$$

where b is the radius of the rotating reactor. For $|\Delta\rho|/\rho_p \sim 0.1$, $g \sim 10^3$ cm/sec^2, $b \sim 3.0$ cm and the above value for c, Ω_{min} is 7.4×10^{-4} sec^{-1}, cf. Table 2.

Using the assumption (24), the two roots of the quadratic equation (16) can be approximated as

$$m_1 = i\Omega + d , \tag{27}$$

$$m_2 = -c - i\Omega \ , \tag{28}$$

where the growth or decay rate for the first spiral, in equation (27), is

$$d = \frac{\Delta\rho}{\rho_p}\frac{\Omega^2}{c} \ , \tag{29}$$

which is real and much less than Ω. Note that for the second spiral, the real part is $-c$, so that the radius decreases exponentially on the very short drag time scale, $1/c$. Thus the second spiral solution becomes negligibly small in a few drag time scales, for any realistic initial conditions. The full general solution therefore can be approximated as

$$x = x_o + \alpha e^{dt} \cos(\Omega t + \theta) \ , \tag{30}$$

$$y = \alpha e^{dt} \sin(\Omega t + \theta) \ , \tag{31}$$

where α and θ are determined by the initial displacement from the center of the spiral.

Note that the radius of the displaement from the spiral center is αe^{dt}, where d is much less than Ω and has the sign of $\Delta\rho$. The rotation rate of the spiral is Ω, so the particle rotates about the center of the spiral at the same rate as the fluid rotates about the axis. The exponent for growth or decay of the radius during the experimental time T is

$$\varepsilon = |d|T = \frac{|\Delta\rho|\Omega^2 T}{\rho_p c} . \qquad (32)$$

Whether $\Delta\rho$ is positive or negative, we will normally require that the exponent ε is of order unity or less, for otherwise either most of the particles spiral out to the boundary of the reactor or they spiral in until their concentration is excessive. Thus we require

$$\Omega^2 < \Omega^2_{max} = \frac{\rho_p c}{|\Delta\rho|T} = \frac{9\eta}{2a^2 T|\Delta\rho|} . \qquad (33)$$

For $T = 10^5$ sec, or slightly larger than a day, the upper limit for Ω using the previous assumptions is 2.12 sec^{-1}.

Physically, the spiralling in or out is caused by the centrifugal force less the inward centrifugal pressure force. That is why it has the sign of $\Delta\rho$. This force is balanced by the drag force to determine the rate of spiralling inwards or outwards.

By equating the lower and upper limits, (26) and (33), for Ω, we can obtain an approximate upper limit for the radius of the particles for the rotating reactor to be useful,

$$a^6_{max} = \left(\frac{9\eta}{2|\Delta\rho|}\right)^3 \frac{b^2}{g^2 T} . \qquad (34)$$

Using $\eta \sim 10^{-2}$ gm/cm sec, $|\Delta\rho| = 0.1$ gm/cc, b = 3 cm, g = 10^3 cm/sec^2 and T = 10^5 sec, as before, we obtain a_{max} as 1.42 x 10^{-2} cm, corresponding to a diameter of 284 μm. This upper limit is further discussed in the following section.

4. OPTIMIZATION OF THE ROTATION RATE

From the previous section, the choice of the rotation rate involves the following dimensionless variables

$$\delta = \frac{|x_o|}{b} = \frac{\Omega_{min}}{\Omega} = \frac{2ga^2|\Delta\rho|}{9b\eta\Omega}, \tag{35}$$

$$\varepsilon = \frac{\phi^3}{2\delta^2} = \left(\frac{\Omega}{\Omega_{max}}\right)^2 = \frac{2a^2T|\Delta\rho|\Omega^2}{9\eta} . \tag{36}$$

Here we have introduced the dimensionless quantity ϕ^3, independent of the rotation rate, and derived by the relations

$$\begin{aligned}
\phi^3 &= 2\varepsilon\delta^2 \\
&= 2(\Omega_{min}/\Omega_{max})^2 \\
&= 2(a/a_{max})^6 \\
&= 2a^6g^2Tb^{-2}\ (2|\Delta\rho|/9\eta)^3 .
\end{aligned} \tag{37}$$

The definition using ϕ^3, and the factor 2, are for later convenience.

The limit Ω_{min} corresponds to the strict requirement

$$\delta < 1, \tag{38}$$

so that the spiral center is inside the rotating reactor. The limit Ω_{max} correspnds to the loose requirement

ORIGINAL PAGE IS OF POOR QUALITY

$$\varepsilon \lesssim 1 \, , \tag{39}$$

so that the centrifugal spiralling is not excessive during the period T. The radius changes by a factor e^{ε} during this time inteval.

An optimization problem can be defined for both signs of the particle density excess $\Delta\rho$. For positive $\Delta\rho$, the particles spiral outward, and we maximize the fraction F of the reactor cross section area for which particles starting there will not hit the reactor wall in the time interval T. For negative $\Delta\rho$, the particles spiral inwards, and we maximize the fraction F of the reactor cross section area containing particles which have not hit the wall in the preceding time interval T. T is much more than a rotation period, and is taken as 10^5 sec (or 27.8 hours) for our examples. Note that this analysis makes no use of the loose inequality (33).

In both cases, the area involved is a circle with its center at the spiral center. The distance from the spiral center to the cylinder wall is $(b-|x_o|)$. The radius of the circle is therefore

$$r_F = (b - |x_o|)e^{-\varepsilon} \, . \tag{40}$$

The fraction F is the ratio of the area of this circle (the smallest circle in Figure 3) to the cylinder cross section area (the largest circle). Thus

$$F = \frac{\pi r_F^{\,2}}{\pi b^2} = (1 - \delta)^2 \, e^{-2\varepsilon}$$

$$= (1 - \delta)^2 \exp\left(- \phi^3/\delta^2\right) \, . \tag{41}$$

ORIGINAL PAGE IS
OF POOR QUALITY

In this last expression for F, ϕ^3 remains constant while Ω and δ vary. F is maximized by differentiation with respect to δ and setting the derivative to zero. Hence

$$\frac{\delta^3}{1 - \delta} = \phi^3 \ . \tag{42}$$

This is a cubic equation in δ, with a single solution in the allowed interval $0 < \delta < 1$, for all positive ϕ values. Approximate analytic solutions for δ can be obtained when ϕ is either very small or very large; otherwise numerical or graphical methods can be used, or δ can be obtained using Table 1 as described below.

Once the optimum δ and F have been found, for a particular set of rotating reactor parameters determining the ϕ^3 values (37), the optimum rotation rate is given by equation (35), in the form

$$\Omega = \Omega_{min}/\delta \ . \tag{43}$$

Using equation (42), with the definitions (35) and (37), this can be written as the alternative form

$$\Omega = \Omega_s \ (1 - \delta)^{-1/3} \ , \tag{44}$$

where

$$\Omega_s = \Omega_{min}/\phi = \left(\frac{g}{2bT}\right)^{1/3} \tag{45}$$

is independent of the particle size and density, and of the fluid properties. For our example, with $g = 10^3$ cm/sec^2, $b = 3$ cm, and $T = 10^5$ sec, Ω_s is 0.118 sec^{-1} or 1.132 rpm. The expression (45) is useful, because $(1 - \delta)^{-1/3}$ does not increase significantly from unity until δ approaches unity.

For the easy case of very small ϕ, Ω_{min} is much less than Ω_{max}. The approximate analytic solution is

$$\delta = \phi \; ,$$

$$\epsilon = \phi/2 \; ,$$

$$F = 1 - 3\phi \; . \tag{46}$$

The corresponding optimum rotation rate for small ϕ is

$$\Omega = \Omega_s \; (1 + \phi/3) \; , \tag{47}$$

or approximately Ω_s. The rotation rate is independent of the particle and fluid properties so long as they ensure that ϕ is small.

The example introduced in the previous section leads to a very small ϕ value. Using those values,

$$\begin{aligned}
\Omega_{min} &= 7.4 \times 10^{-4} \ \sec^{-1} \ , \\
\Omega_{max} &= 2.12 \quad \sec^{-1} \ , \\
\phi^3 &= 2(\Omega_{min}/\Omega_{max})^2 = 2.44 \times 10^{-7} \ , \\
\delta &= \phi = 0.00625 \ , \\
\varepsilon &= \phi/2 = 0.00312 \ , \\
F &= 1 - 3\phi = 0.9813 \ ,
\end{aligned} \tag{48}$$

The optimum rotation rate is accurately given by equation (47), and is almost exactly Ω_s. The spiral center is at

$$|x_o| = b\delta = 0.019 \text{ cm} \ , \tag{49}$$

which is an imperceptible displacement from the reactor axis.

On the other hand, the approximate solution for large ϕ is

$$\begin{aligned}
\delta &= 1 - \phi^{-3} \ , \\
\varepsilon &= \phi^3/2 \ , \\
F &= \phi^{-6} \exp(-\phi^3) \ .
\end{aligned} \tag{50}$$

This is the hard case of large particles, with Ω_{min} much greater than Ω_{max}. The optimum Ω is only slightly larger than Ω_{min}, and the particles centrifuge so rapidly that the fraction F is exponentially small, and the Rotary Reactor is in effect useless.

For intermediate values of ϕ^3, as given by equation (37), the use of Table 1 may be preferable to solving the cubic equation (42), particularly since F is insensitive to δ near the optimum value. The table shows optimal values of δ spaced uniformly from zero to one, with the corresponding values of

$$\phi^3 = \delta^3/(1 - \delta) \ ,$$

$$\varepsilon = \phi^3/2\delta^2 \ ,$$

$$F = (1 - \delta)^2 \, e^{-2\varepsilon} \ ,$$

$$(1 - \delta)^{-1/3} \ .$$

The table can be used, with hand interpolation, to determine values for the other parameters, assuming an optimized rotation rate, for any value of ϕ^3 (or of ε or F).

To illustrate the application of Table 1, consider the example given in the previous section for which the radius is calculated using $\Omega_{max} = \Omega_{min}$. This gives in succession

$$a = a_{max} = 1.42 \times 10^{-2} \text{ cm},$$

$$\Omega_{max} = \Omega_{min} = 2^{1/3}\ \Omega_s = 0.1494 \text{ sec}^{-1} ,$$

$$\phi^3 = 2 ,$$

$$\delta = 0.77 ,$$

$$\varepsilon = \phi^3/2\delta^2 = 1.68 ,$$

$$F = (1 - \delta)^2 \exp(-2\varepsilon) = 0.0013 ,$$

$$\Omega = \Omega_{min}/\delta = \Omega_s/(1 - \delta)^{1/3} = 0.1939 \text{ sec}^{-1} .$$

Here δ is obtained from ϕ^3 by interpolation in the table, and ε and F are then obtained from the formulas. The fraction F of the particles not hitting the wall is unacceptably small, even at the optimum rotation radius.

To determine the largest radius for which a fraction F of 0.5 can be obtained, we again look to the table, and obtain approximately,

$$\delta = 0.2 ,$$

$$\phi^3 = 0.01 .$$

From equation (37),

$$(a/a_{max})^6 = \phi^3/2 = (0.4135)^6$$

which gives a radius limit of 5.9×10^{-3} cm (corresponding to a diameter of 117 μm) for our example. The corresponding optimum rotation rate is

$$\Omega_s/(1 - \delta)^{1/3} = 0.1278 \text{ sec}^{-1} .$$

5. CONCLUSIONS

A rotary reactor is a cylinder of fluid rotating about its horizontal axis in order to keep particles in suspension. Such a reactor has been used to produce larger latex microspheres in the laboratory without flocculation, with results approaching those obtained in space.

An accurate solution for the path followed by a particle in a rotating reactor has been obtained. The path depends on whether the particle is heavier or lighter than the fluid. For counterclockwise rotation, a heavy particle spirals outwards around a spiral center displaced to the right of the axis. A light particle spirals inwards around a center displaced to the left. The spiral rotation rate is the same as the rotation rate of the reactor. The relative change in the radius, for each spiral rotation, is very small.

Physically, the horizontal displacement of the spiral center from the axis of rotation is determined by the condition that the net weight or buoyancy should balance the viscous drag from the fluid flow past the particle. The spiralling outwards or inwards is due to the centrifugal buoyancy (i.e. the centrifugal force on the particle as compared with the centrifugal force on the fluid it displaces).

There are two constraints on the rotation rate of the reactor. It must exceed the minimum value (26), to keep the spiral center inside the reactor. And it must not be much larger than the maximum value (33), since either too many particles hit the reactor wall or the particle concentration becomes excessive (for light particles spiralling inwards).

For both cases, there is a natural optimization problem, to choose the rotation rate to maximize the fraction of the reactor cross section area which contains particles which either will not spiral out to the reactor wall during the experimental time, or have spiralled in without hitting the wall.

The optimization problem was solved, to determine the optimum rotation rate and the corresponding fraction value, for any set of parameters. Remarkably, the optimum rotation rate is independent of the particle and fluid properties, for small particles, and increases only a little as the particle size increases.

Table 2 presents the parameter values for the three examples used in the text. The fluid properties, density difference, reactor diameter, and experimental time are the same in each case. Particle diameters in micrometers of 20, 284, and 117 are considered. The computed rotation rates are presented in rpm units for engineering convenience. The optimum rotation rate maximized the success fraction F of the reactor cross section area. The spiral center displacements (from the reactor axis) are shown. The distance of each particle from the spiral center changes by the indicated factor during the experimental time.

For the first column, the particle diameter was chosen as a typical value of interest. The minimum rotation rate is much less than the nominal maximum, and a high success fraction is obtained, with a small spiral center displacement and a radius change factor close to unity.

In the second column, the particle diameter was chosen to make the maximum and minimum rotation rates equal. The optimum rotation rate is somewhat higher, the spiral center is near the reactor wall, the radius changes by a factor of over five, and the success fraction is very small.

For the third column, the particle diameter was chosen to give a success fraction of a half. The other parameter values are shown.

The time T in the table is roughly appropriate for latex microsphere processing. Note that the optimum rotation rate given by equation (44) and (45) varies only with the one-third power of g/[illegible]T, and is practically independent of the particle radius and density, provided (37) is small. Thus the optimum rotation rate is close to rpm for latex microspheres, and is probably between 0.1 rpm and 10 rpm for a very wide range of microgravity simulations.

Further work is required for a full application of this analysis to the production of monodisperse latex microspheres. As described in Section 1, the monomer-swollen seed particles are buoyant in the early stages, and converge on the spiral center. In the later stages, the particles shrink slightly and become heavier than water, and the spiral center crosses the axis. The heavier particles centrifuge out as the polymerization approaches completion.

The risk and extent of coagulum formation during this process, and the deviations from a monodisperse size distribution due to variations in the particle distribution, are unknown. It can be expected that even if the particles collide near the spiral center as they centrifuge in during the early stages, the forces between the particles will be much smaller than for particles creamed to the top in a non-rotating reactor. This is because the centrifugal accelerations are extremely small. Thus coagulum formation might be minimal. In the late stages, as particles centrifuge out and hit the wall, there will be further particle collisions, with again the possibility of coagulum formation or size dispersion.

A further issue involves the beginning of production, and the dynamics and thermodynamics of raising the temperature, with or without stirring. The stirring could also be continued into the polymerization stage.

Finally, we assumed that the solid-body rotation of the fluid is not disturbed by the presence of the particles. However, recent experiments by Kornfeld show significant secondary flows driven by concentration variations, for 0.3% suspensions of 50 micron latex particles, at rotation rates below 1 rpm. The dependence of this phenomenon on concentration is weak, while its dependence on rotation rate is very abrupt; at 1.4 rpm there is no observable modification from uniform rotation, while at 0.7 rpm the flow field and particle distribution are totally different. We plan further study of this effect.

REFERENCES

1. Vanderhoff, J. W., Preprints, Org. Coatings Plastics Cham. 24 (2), 223 (1964).

2. Vanderhoff, J. W., El-Aasser, M. S., and Micale, F. J., Abstracts, 175th ACS Meeting, Anaheim, CA, March 13-17, 1978, COLL-110.

3. Vanderhoff, J. W., El-Aasser, M. S., Kornfeld, D. M., Micale, F. J., Sudol, E. D., Tseng, C.-M., and Sheu, H.-R., Mat. Res. Soc. Symp. Proc., 87, 213-223 (1987).

4. Kornfeld, D. M., "Monodisperse Latex Reactor - A Materials Processing Space Shuttle Mid-Deck Payload," NASA TM-86487, Marshall Space Flight Center, Alabama, January 1985.

5. U.S. Patent No. 4,247,434; issued January 27, 1981, "Process for Preparation of Large-Particle-Size Monodisperse Latexes," Inventors: Vanderhoff, J. W., Micale, F. J., El-Aasser, M. S., and Kornfeld, D. M.

6. Otto, G. H., and Lorenz, A., "Simulation of Low Gravity Conditions by Rotation." AIAA Paper Number 78-273, 1978.

7. Schatz, A., "Problems of 0-g Simulation With the Fast-Running Clinostat." Institute for Aerospace Medicine, Cologne, Germany.

8. Dill, L.H. and Brenner, H., J. Colloid Interface Sci. 94, 430. (1983)

9. Nadim, A., Cox, R.G. and Brenner, H., Phys. Fluids 28, 3457 (1985).

10. Aoki, A., Shirane, K., Tokimoto, T. and Nakagawi, K., Rev. Sci. Instrum. 57, 2859 (1986).

11. Annamalai, A. and Cole, R., Adv. Space Res. 3, 165 (1983).

12. Annamalai, A. and Cole, R., Adv. Space Res. 8, 321 (1987).

Table 1. Parameter Values Corresponding to Uniformly Spaced δ Values

δ	ϕ^3	$e^{-\varepsilon}$	F	$(1-\delta)^{-1/3}$	δ	ϕ^3	$e^{-\varepsilon}$	F	$(1-\delta)^{-1/3}$
0.05	.00013	0.974	0.856	1.017	0.50	0.250	0.6065	0.0920	1.260
0.10	.00111	0.946	0.725	1.036	0.55	0.370	0.5427	0.0597	1.305
0.15	.00397	0.916	0.606	1.056	0.60	0.540	0.4724	0.0357	1.357
0.20	.0100	0.882	0.498	1.077	0.65	0.785	0.3851	0.0191	1.419
0.25	.0209	0.846	0.403	1.101	0.70	1.143	0.3114	0.0087	1.494
0.30	.0386	0.807	0.319	1.126	0.75	1.687	0.2231	0.0031	1.587
0.35	.0660	0.764	0.247	1.154	0.80	2.560	0.1353	0.0007	1.710
0.40	0.1067	0.717	0.185	1.186	0.85	4.094	0.0588	0.0001	1.882
0.45	0.1657	0.664	0.133	1.221	0.90	7.290	0.0111	10^{-6}	2.154

Parameter	Equation	Explanation
δ	(35)	Spiral center, scaled by the ractor radius b, for the optimized rotation rate.
ϕ^3	(37)	Problem parameter, proportional to sixth power of the particle radius a.
$e^{-\varepsilon}$	(36)	Spiral radius changes by factor e^{ε} during time T.
F	(41)	Area occupied by particles not interacting with reactor wall during time T, as fraction of reactor cross section. Maximized value.
$(1-\delta)^{-1/3}$	(44)	Optimum rotation rate, scaled by $\Omega_s = (g/2bT)^{1/3}$.

Table 2. Typical Parametric Values to Illustrate Rotation Rate Limits

Quantity	Symbol	Values			Unit
Particle Diameter	2a	20	284	117	μm
Water Viscosity	η	0.01	0.01	0.01	gm/cm/sec
Water Density	ρf	1	1	1	gm/cc
Density Difference	$\Delta\rho$	0.1	0.1	0.1	gm/cc
Reactor Diameter	2b	6	6	6	cm
Experimental Time	T	10^5	10^5	10^5	sec
Rotation Rate Minimum	Ω_{min}	0.0071	1.43	0.243	rpm
Nominal Rotation Rate Maximum	Ω_{max}	20.2	1.43	8.43	rpm
Optimum Rotation Rate	Ω	1.13	1.85	1.22	rpm
Spiral Center Displacement	x_o	0.019	2.31	0.60	cm
Radius Change Factor	$e^{-\epsilon}$	0.997	0.186	0.882	--
Optimized Success Fraction	F	0.981	0.0018	0.500	--

FIGURE CAPTIONS

Figure 1. A prototype Rotary Reactory to minimize gravitational settling (or creaming) for the growing latex particles.

Figure 2. Schematic view along the axis of symmetry of the Rotary Reactor showing the coordinate system used.

Figure 3. Cross-section of the rotary reactor. Heavy or light particles at A are stationary, supported against gravity by the counterclockwise or clockwise flow. Other particles move around A in circles, spiralling slowly outward or inward. Particles in the crescent hit the wall on the first cycle. Heavy particles initially between the concentric circles spiral out to hit the wall in time T. Heavy particles in the inner circle spiral out to fill the outer circle. Light particles initially filling the outer circle fill the inner circle after time T. In both cases we choose the rotation rate to maximize the area of the inner circle.

ROTARY REACTOR

CHAMBER FLUID CAPACITY: 235 ml
CHAMBER MATERIALS: ALL STAINLESS STEEL WITH PYREX WALLS, AND VITON O- RING SEALS

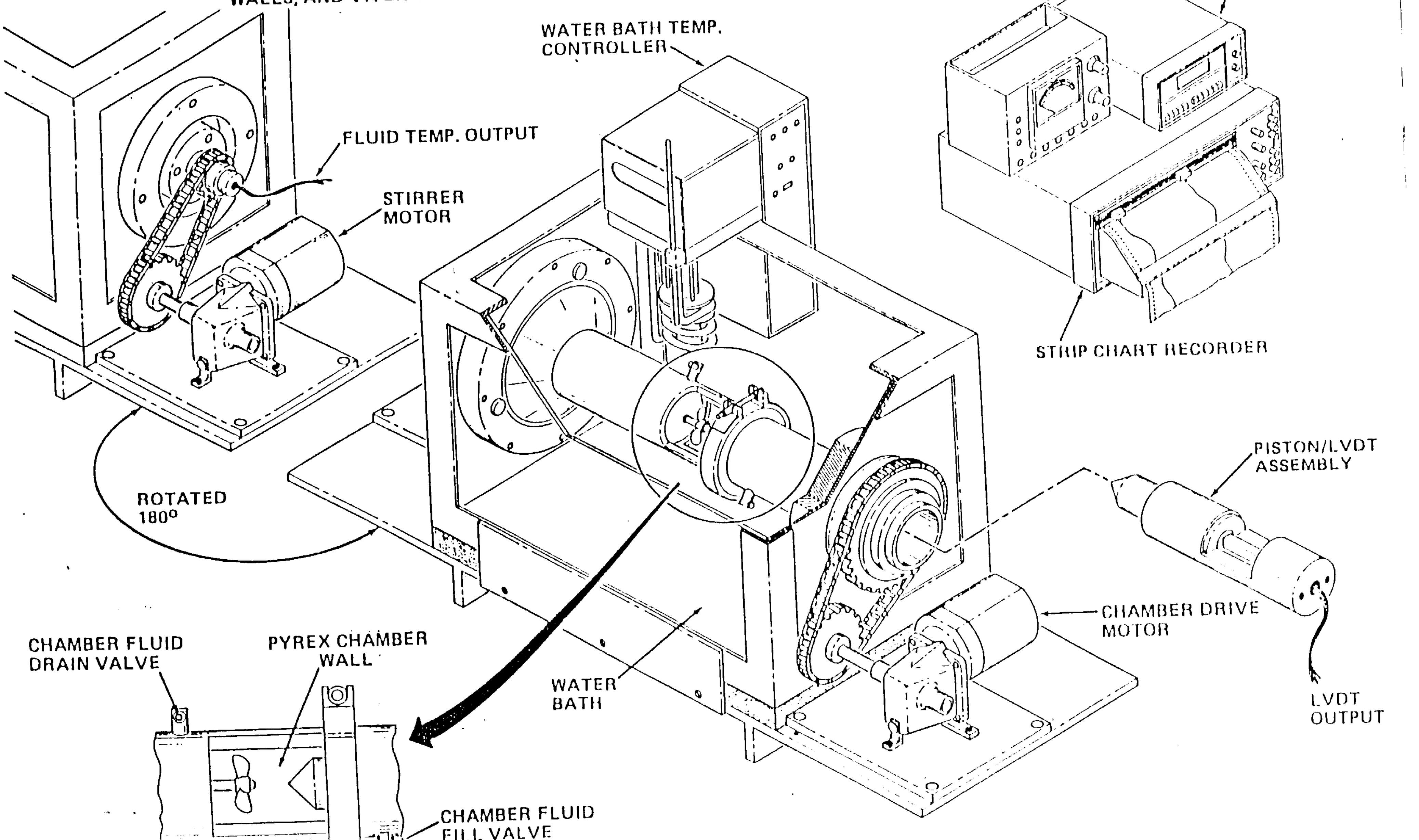

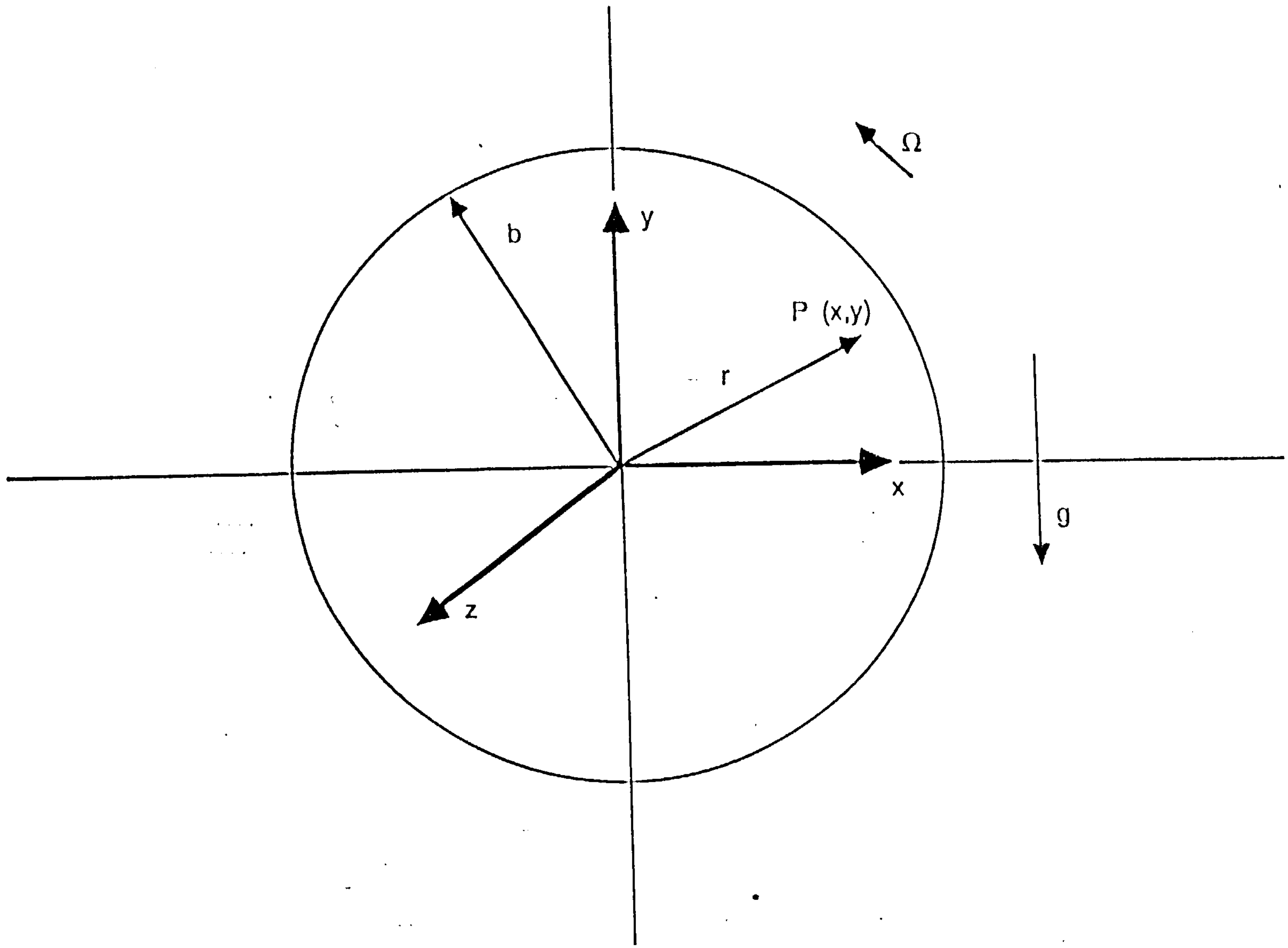

5-791-7-11

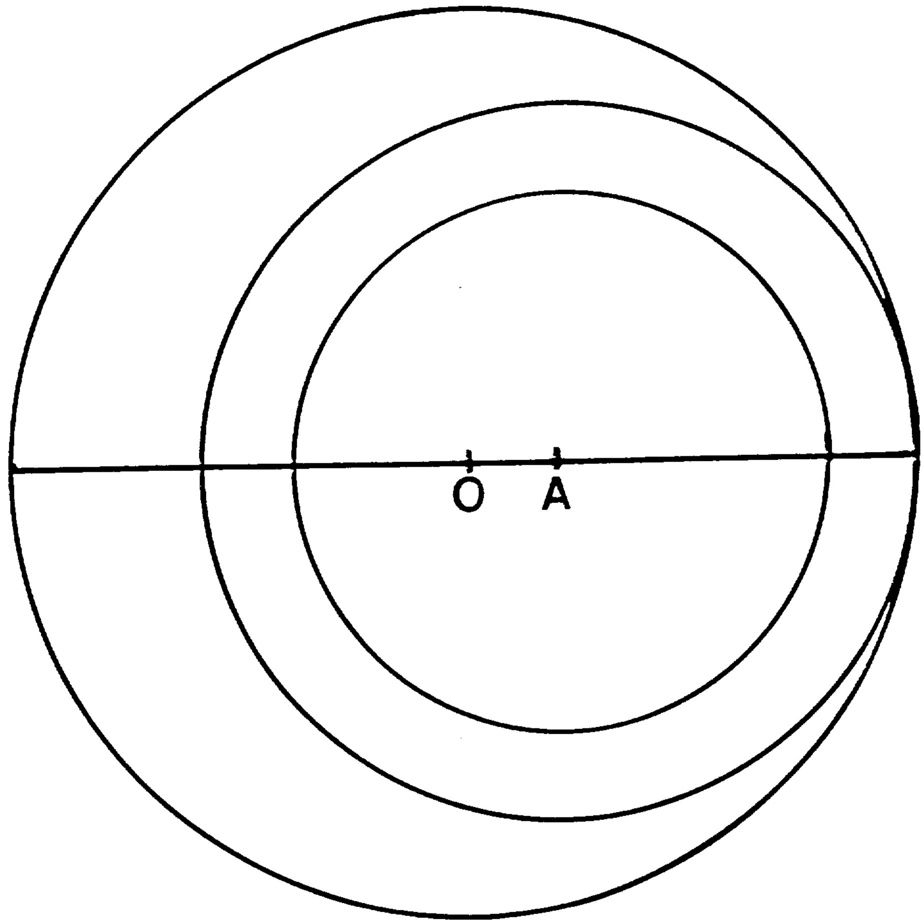
O
A

NASA
National Aeronautics and Space Administration

Report Documentation Page

1. Report No.	2. Government Accession No.	3. Recipient's Catalog No.
4. Title and Subtitle Rotating Reactor Studies		5. Report Date 1/91
		6. Performing Organization Code
7. Author(s) Glyn O. Roberts		8. Performing Organization Report No. RAI-89-RR-2
		10. Work Unit No.
9. Performing Organization Name and Address Roberts Associates, Incorporated 380 West Maple Avenue, Suite L-1A Vienna, VA 22180-5616		11. Contract or Grant No. P/O H-80505B
		13. Type of Report and Period Covered Final
12. Sponsoring Agency Name and Address National Aeronautics and Space Administration, Washington, DC 20546-0001 George C. Marshall Space Flight Center		14. Sponsoring Agency Code

15. Supplementary Notes

16. Abstract

Rotating Reactors can be used to simulate fluid processes in microgravity.

This is a final report on studies related to particle orbits in the uniformly rotating fluid in such a reactor.

Our prior analysis of particle orbits is expanded. An optimization problem is defined and solved, to determine an optimum rotation rate to keep particles in solution for a long period. Computer graphics are used to demonstrate the optimization.

17. Key Words (Suggested by Author(s))	18. Distribution Statement
Rotating reactor Particle Orbits, Centrifugal Buoyancy Polystyrene Latex Particles	Unclassified-Unlimited Subject Category 29 Materials Processing

19. Security Classif. (of this report)	20. Security Classif. (of this page)	21. No. of pages	22. Price
Unclassified	Unclassified	74	

NASA FORM 1626 OCT 86